INSTITUTE OF PHYSICS PUBLISHING REPORTS ON PROGRESS IN PHYSICS

Rep. Prog. Phys. **68** (2005) 2665–2700 doi:10.1088/0034-4885/68/11/R04

Computer simulation of liquid crystals

C M Care and D J Cleaver

Materials and Engineering Research Institute, Sheffield Hallam University, Howard Street, Sheffield, S1 1WB, UK

E-mail: c.m.care@shu.ac.uk and d.j.cleaver@shu.ac.uk

Received 5 August 2002, in final form 8 August 2005
Published 12 September 2005
Online at stacks.iop.org/RoPP/68/2665

Abstract

A review is presented of molecular and mesoscopic computer simulations of liquid crystalline systems. Molecular simulation approaches applied to such systems are described, and the key findings for bulk phase behaviour are reported. Following this, recently developed lattice Boltzmann approaches to the mesoscale modelling of nemato-dynamics are reviewed. This paper concludes with a discussion of possible areas for future development in this field.

(Some figures in this article are in colour only in the electronic version)

Contents

1. Introduction

In this paper, we review molecular and mesoscopic computer simulations of liquid crystalline (LC) systems. Owing to their ability to form LC mesophases, the molecules of LC materials are often called mesogens. Following a scene setting introduction and a brief description of the key points of LC behaviour, we first review the application of molecular simulation approaches to these mesogenic systems; we only consider bulk behaviour and do not report work on confined or inhomogeneous systems. This section is largely broken down by model-type, rather than area of application, and concentrates on the core characteristics of the various models and the results obtained. In contrast, in section 4, we give relatively detailed descriptions of a series of recently developed lattice Boltzmann (LB) approaches to LC modelling and nemato-dynamics—following a period of relatively rapid development, a unifying review of this area is particularly timely. Finally, in section 5, we identify a number of key unresolved issues and suggest areas in which future developments are likely to make most impact.

Note that we do not review results obtained using conventional solvers for the continuum partial differential equations of LC behaviour. Whilst it might legitimately be argued that the mesoscopic technique considered in this review, LB, is simply an alternative method of solving the macroscopic equations of motion for the LCs, this particular method is perhaps best thought of as lying on the boundary between macroscopic and molecular methods. Additionally, it is straightforward to adapt the LB method to include additional physics (e.g. the moving interfaces found in LC colloids); as such, a clear distinction can be drawn between the LB approaches reviewed in section 4 and conventional continuum solvers.

Previous reviews of LC simulation include the general overviews by Allen and Wilson (1989) and Crain and Komolkin (1999) and a number of other works which concentrate on specific classes of model. For hard particle models, the papers by Frenkel (1987) and Allen (1993) offer accessible alternatives to the all-encompassing Allen *et al* (1993). Zannoni's (1979) very early review of lattice models of LCs has now been significantly updated by Pasini *et al* (2000a) in a NATO ARW proceedings (Pasini *et al* 2000b) which contains some other useful overview material, while Wilson (1999) has summarized work performed using all-atom models. Finally, there are two accessible accounts of work performed using generic models—Rull's (1995) summary of the studies that enabled initial characterization of the Gay–Berne mesogen and the more recent overview by Zannoni (2001) which cogently illustrates subsequent developments and diversifications.

1.1. The role of computer simulation in liquid crystal research

Computer simulation is simply one of the tools available for investigating mesogenic behaviour. It is, however, a relative newcomer compared with the many experimental and theoretical approaches available, and its role is often complementary; there is little to be gained from simulating a system which is already well characterized by more established routes. That said, appropriately focused computer simulation studies can yield a unique insight into molecular ordering and phase behaviour and so inform the development of new experiments or theories. Most obviously, molecular simulations can provide systematic structure property information, through which links can be established between molecular properties and macroscopic behaviour. Alternatively, simulation can be used to test the validity of various theoretical assumptions. For example, by applying both theory and simulation to the same underlying model, uncertainties regarding the treatment of many-body effects in the former can be quantified by the latter.

One of the strengths of simulation in the context of LCs arises in situations for which there are (spatial or temporal) gradients in key quantities such as the order tensor or the

composition profile. Such gradients are often difficult to resolve experimentally and are only accessible to relatively coarse-grained theories. In comparison, computer simulation of 'gradient regions' can often be achieved at the same computational cost as that needed to treat 'uniform regions'; in these contexts, therefore, simulation is becoming the lead complementary technique for improved understanding of behaviours which are not fully accessible to experimental investigation.

At continuum length scales, LCs are characterized by a large number of experimentally observable parameters: viscosities, determined by the Leslie coefficients; orientational elasticity, controlled by the Frank constants; substrate–LC orientational coupling, governed by anchoring coefficients and surface viscosities. Given a full set of these parameters, mesoscale simulations are now able to incorporate much of this complex behaviour into models of real devices. Thus, subject to the usual provisos concerning continuum models, these approaches are now starting to gain the status of design and optimization tools for various LC device applications.

Before presenting the details of this review, we first ask the rather fundamental question—why perform computer simulations of LCs? LCs are fascinating systems to study because, like much of soft-condensed matter, their behaviour is characterized by the interplay of several very different effects which operate over a wide range of time- and length-scales. These effects range from changes in intra-molecular configurations, through molecular librations to many-body properties such as mass flow modes and net orientational order and ultimately to the fully equilibrated director field observed at the continuum time- and length-scales. The extent of the associated time- and length-scale spectra dictate that no single computer simulation model will ever be able to give a full 'atom-to-device' description for even the simplest mesogen. Moreover, since these different phenomena are, in general, highly coupled (e.g. intramolecular configurations are influenced, in part, by the local orientational order), they represent a multi-level feedback system rather than a simple linear chain of independent links. Thus, addressing each phenomenon with its own model and simply collating the outputs of a series of stand-alone studies will again fail to achieve a full description. In partial recognition of this, most of the methods and models currently used to simulate LCs seek to explore only a subset of the spectrum of behaviours present in a real system. In some cases, this pragmatic approach is entirely appropriate: for certain bulk switching applications, for example, a continuum description can prove perfectly adequate (explaining the popularity of Ericksen–Leslie theory), and the molecular basis of LCs can be neglected. Alternatively, a well defined generic model approach can provide the cleanest route to establishing relationships between molecular characteristics and bulk properties such as the Frank constants or the Leslie coefficients. Returning to the original question, then, we can reply that appropriately focused simulation studies have certainly provided a sound understanding of many of the processes underlying bulk mesogenic behaviour and the operation of some simple switching devices.

The role of computer simulations in studying LCs is relatively well established; as noted above and shown in more detail in the following sections, successful approaches have now been developed for many of the regions in the atom-to-device spectrum. As such, several of the fundamental problems in this field are now essentially solved. Given these achievements, it is now appropriate to raise the supplementary question—why continue to perform computer simulations of LCs? There is little of note to be gained by simply refining existing approaches and exploiting Moore's law to incrementally enlarge the scope of, say, three-dimensional bulk simulations of generic LC models of conventional thermotropic behaviour. Many of the outstanding challenges in LC science and engineering call, instead, for either predictive modelling, needed to make simulation an effective design tool for device engineers, or simulation methodologies capable of describing 'butterfly's wings' problems, in

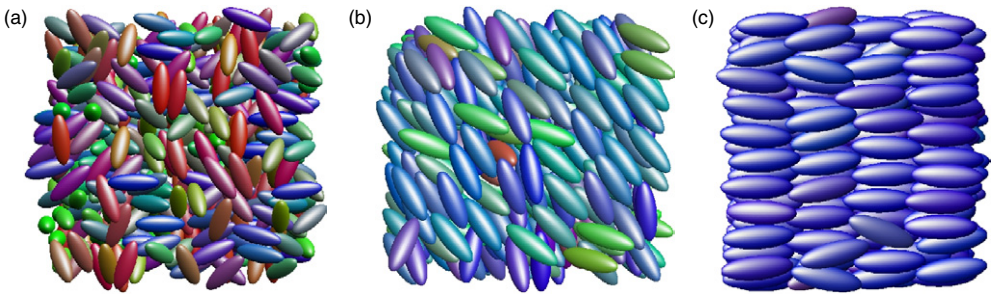

Figure 1. (*a*) Isotropic, (*b*) nematic and (*c*) smectic phases (configurations obtained from simulations performed using the Gay–Berne mesogen).

which processes acting at molecular length-scales induce responses at the macroscale. Whilst addressing these classes of problem may require some development of new models, a more pressing need comes from the lack of adequate hybrid methodologies, i.e. two-way interfaces between existing classes of model. Indeed, the maturity of the field of LC simulation and the problems still posed to it mark it out as an ideal test-bed for moving established (but largely independent) models on to another level through the development of novel integrated simulation methodologies.

As indicated above, the remainder of this paper is arranged as follows. In the next section, we give a very brief introduction to the field of LCs. We then review molecular simulations of LC behaviour, and mesoscopic LB approaches to nemato-dynamics, before concluding with suggestions for possible future developments.

2. Materials and phases

The LC phases are states of matter that exist between the isotropic liquid and crystalline solid forms in which the molecules have orientational order but no, or possibly partial, positional order. Particles which are able to form LC phases are called mesogenic; hence the term mesogen is used to refer to a molecule that forms a mesophase or LC phase. Typically, mesophases have some material properties associated with the isotropic liquid (ability to flow, inability to resist a shear) and others more commonly found in true crystals (long range orientational and, in some cases, positional order, anisotropic optical properties, ability to transmit a torque). The term LC actually encompasses several different phases, the most common of which are nematic and smectic; these are described at length in the classic texts dedicated to LCs (Chandrasekhar 1992, deGennes and Prost 1993, Kumar 2001) and in a recently published collection of some of the key early research papers (Sluckin *et al* 2004).

Most mesogens are either calamitic (rod shaped) or discotic (disc like); a sufficient (though not necessary) requirement for a substance to form a mesophase is a strong anisotropy in its molecular shape. Typically, calamitic mesogens contain an aromatic rigid core, formed from, e.g. 1,4-phenyl or cyclohexyl groups, linked to one or more flexible alkyl chain(s). In families of LCs, the variants with short alkyl chains tend to be nematogens (mesogens that form nematic phases), while those with longer alkyl chains are smectogens (mesogens that form smectic phases).

The nematic phase is the simplest LC phase and is characterized by long range orientational order but no long range translational order. In the nematic phase (figure 1(*b*)), correlations in molecular positions are essentially the same as those found in an isotropic fluid, but the molecular axes point, on average, along a common direction, the director $\hat{\mathbf{n}}$. In the usual case

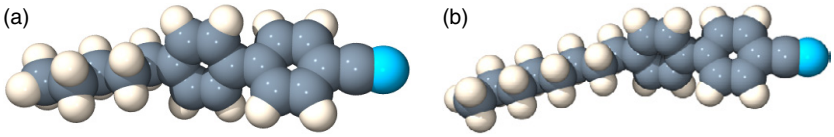

Figure 2. Molecules of 4-pentyl-4′-cyanobiphenyl (5CB) and 4-octyl-4′-cyanobiphenyl (8CB) molecules.

of a nematic phase with a zero polar moment, the symmetry properties of the phase remain unchanged upon inversion of the director. If chiral molecules are used (or a chiral dopant is introduced), a cholesteric or chiral nematic phase can be obtained. The difference between this and the standard nematic phase is that in the former, the director twists as a function of position, but with a pitch which is much larger than molecular dimensions.

The smectic phases are characterized by long range translational order, in one or two dimensions, as well as long range orientational order. Thus, in smectic phases (figure 1(*c*)), in addition to having a director, the molecules are arranged in layers. Depending on the angle between the director and the layer normal, and details of any in-plane positional ordering, numerous different smectic phases have been hypothecated. In practice, however, in computer simulation studies it is often impossible to distinguish these phases from one another or from the underlying crystalline solid phase.

The stability of LC phases can often be enhanced by increasing the length and polarizability of the molecule or by the addition of, e.g. a terminal cyano group to induce polar interactions between the molecule pairs. Lateral substituents can also influence molecular packing. For example, incorporating a fluoro group at the side of the rigid core can enhance the molecular polarizability but disrupt molecular packing, leading to a shift in the nematic–isotropic (N–I) transition. Creating a lateral dipole in this way can also promote formation of tilted smectic phases and, in the case of chiral phases, give rise to ferroelectricity. Further details regarding the effects of various molecular features on nematic behaviour can be found in Dunmur *et al* (2001).

The classic example of a room-temperature mesogen is the *n*-cyanobiphenyl or *n*CB family shown in figure 2. Here the rigid core is made of a meta biphenyl unit; at one end of this core is the flexible tail, an alkyl chain of n carbons (C_nH_{2n+1}), while at the other is the polar cyano head group. The influence of the alkyl chain length is apparent from a comparison of the phase sequences for 5CB and 8CB.

$$\begin{aligned} &\text{5CB}: \quad \text{crystal}^{23\,^\circ\text{C}} \rightarrow \text{nematic}^{35\,^\circ\text{C}} \rightarrow \text{isotropic},\\ &\text{8CB}: \quad \text{crystal}^{21^\circ\text{C}} \rightarrow \text{smectic A}^{32.5\,^\circ\text{C}} \rightarrow \text{nematic}^{40\,^\circ\text{C}} \rightarrow \text{isotropic}. \end{aligned}$$

For molecules such as HHTT (figure 3), in which one of the molecular axes is significantly *shorter* than the other two, the alternative family of discotic phases can arise. Discotic mesogens typically have a core composed of aromatic rings connected in an approximately circular arrangement from which alkyl chains extend radially. In the discotic nematic phases, the director is the average orientation of the *short* molecular axes. As with the smectic phases, several types of columnar discotic arrangement have been suggested, the characterization relating to column–column correlations and the relationship between orientational and positional symmetry axes. Again, though, distinguishing between these different columnar phases is generally beyond the capabilities of current simulation models.

In addition to these classic thermotropic calamitic and discotic systems, several other forms of LC behaviour are known. For example, there are numerous experimentally established systems—such as LC polymers and lyotropic LCs—which involve some level of mesogenic behaviour. Also, recent years have seen growing interest in the design and examination of

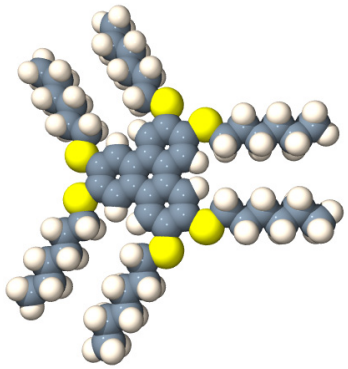

Figure 3. Molecular representation of the HHTT molecule (2,3,6,7,11-hexahexylthiotriphenylene).

alternative classes of mesogenic molecule (see, e.g. Tschierske (2001)). Thus, various families of 'bent' (or 'banana-shaped') and 'tapered' (or 'pear-shaped') molecules have recently been synthesized with the aim of inducing exotic behaviour such as biaxial (Acharya *et al* 2004, Madsen *et al* 2004), and ferroelectric nematic phases and enhanced flexoelectricity.

Finally, before closing this section, it is relevant to note that virtually all of the mesogenic materials used in practical applications are multi-component formulations, typically comprising a dozen or more molecule types. Broadly speaking, the prevalence of multi-component systems is explained by the relative ease with which they can be used to relocate phase transition points and selectively modify material properties. The issue of formulation has only recently become accessible to simulation studies, however.

3. Molecular simulations of liquid crystals

3.1. Molecular simulation techniques

The burgeoning field of molecular simulation underpins all of the work described in this section, and so a brief summary of its key components is appropriate. Due to obvious space constraints, a full overview is not possible, and we strongly recommend the standard texts (Allen and Tildesley 1986, Rapaport 1995, Frenkel and Smit 2002) to the interested reader. Here, we restrict ourselves to a brief discussion of the approaches adopted, with the intention of illustrating what is and what is not available on the molecular simulator's palette.

Just as each experimental technique is restricted to a certain time- and length-scale window, so different simulation approaches are able to probe different sets of observables. As such, the choice of appropriate model type(s) and simulation technique(s) is crucial in any project: this is driven by the scientific problem of interest and tempered by knowledge/understanding of the limitations imposed by, e.g. the computational resources available and the range of applicability of the different models considered.

Any molecular simulation has, at its heart, an interaction potential which represents, to some level of approximation, the microscopic energetics that define the simulated system. As we shall see in the following subsections, a range of interaction potentials have been developed for simulating LC behaviour; these are all classical (i.e. they take no direct account of quantum mechanical effects) and based on one- and two-body interactions plus, in some cases, some higher order intramolecular terms. The sum of these contributions is then taken to give the total potential energy of the system. In order to define the system fully, it is also necessary to impose an appropriate thermodynamic ensemble.

Once an interaction potential and the associated thermodynamic conditions have been decided upon, the task for the simulator is commonly to evolve the system configuration from its starting point to its equilibrium state. Once equilibrated, the objective becomes generating a series of representative particle configurations from which appropriate system observables can be measured and averaged. If, as is often the case, only static equilibrium properties are required, a broad range of techniques can be used to perform these equilibration and production stages. By far the most common of these are molecular dynamics (MD) and Monte Carlo (MC) methods.

In an MD simulation, the net force and torque acting on each interaction site are used to determine the consequent accelerations. By recursively integrating through the effects of these accelerations on the particle velocities and displacements, essentially by applying Newton's laws of motion over short but discretized time intervals, the micro-mechanical evolution of the many-body system can be tracked within an acceptable degree of accuracy. Since it mimics the way in which a real system evolves, an MD simulation *can* be used to calculate dynamic properties (such as diffusion coefficients) as well as static equilibrium observables. Its strict adherence to microscopic dynamics means, however, that in some situations (e.g. bulk phase separation) MD does not offer the most efficient route to the equilibrium state; in such situations, MC methods often prove preferable.

In an MC simulation, the microscopic processes (e.g. the particle moves) through which the simulated system evolves are limited only by the simulator's imagination—in principle, any type of move may be attempted, though some will prove more effective than others. For example, in the case of phase separation raised above, particle identity-swap moves can be considered. Despite this free rein in terms of the attempted moves made, adherence to the laws of statistical mechanics is ultimately ensured through the rules by which these moves are either accepted or rejected. Essentially, these rules are imposed such that, once the system has equilibrated, there is a direct relationship between run-averaged observable measurements and the static properties of interest. Thus, while MC simulations routinely use random numbers in the generation of new configurations, the statistical mechanical framework within which these random moves are set ensures that any averages calculated are equivalent to those that would have been obtained using another equilibrium simulation method (such as MD).

Most molecular simulations of LCs, be they MD or MC, involve the translation and/or rotation of interaction sites, processes that are well described by the formalism of rigid-body mechanics (Goldstein *et al* 2002). The mechanical scheme adopted depends on the symmetry and flexibility of the model used but can, in some cases, require the use of quaternions (Allen and Tildesley 1986) rather than the conventional direction cosine description. Additionally, the director constraint approach introduced by Sarman (1996) can prove a useful tool when using MD simulations to investigate long length-scale phenomena. Most LC simulations involve either bulk systems requiring three-dimensional periodic boundary conditions (PBCs) or some combination of PBCs and confining walls (in one or more direction), the latter usually being imposed as a static force field. While cubic simulation boxes are adequate for isotropic and nematic fluids, it has been shown (Domínguez *et al* 2002) that the pressure tensor can become anisotropic at the onset of smectic order unless the box length ratios are allowed to vary.

Calculation of the key orientational observables—the nematic order parameter and director—is commonly based on the order tensor methodology described in the appendix to Eppenga and Frenkel (1984), although an alternative method, based on long range orientational correlations (see Zannoni (1979)), is useful in some situations. For systems in which small numbers of particles are available for order parameter calculations (e.g. when calculating order parameter profiles in confined systems) the systematic overestimation inherent in these

standard methods can become problematic. In such situations, it can prove beneficial to compensate directly for this systematic effect (Wall and Cleaver 1997) or calculate run-averages of orientational order with respect to some box-fixed axis (e.g. the substrate normal). Procedures have also been established for the measurement of higher rank order parameters (Zannoni 2000) and phase biaxiality (Allen 1990).

The onset of smectic order is signalled by mid-range features in the radial distribution function $g(\mathbf{r})$. The extent and in-plane structure of untilted smectic phases can be seen more clearly by resolving this function parallel and perpendicular to the director; smectic A and smectic B phases can be distinguished by the non-zero bond-orientational order found in the latter (Halperin and Nelson 1998). For tilted smectics, where the director is of little use when determining the layer normal, alternative schemes have been developed for projecting out the in-plane and out-of-plane components of $g(\mathbf{r})$ (de Miguel *et al* 1991b, Withers *et al* 2000) and determining the direction of tilt.

3.2. All-atom simulations

Conventionally, molecular simulation is dominated by models based on psuedo-atomistic representations of the molecules found, experimentally, to display the relevant type of behaviour. In the field of LC phase behaviour, however, all-atom models do *not* dominate: instead, the various generic models described in section 3.3 are far more prevalent.

While all-atom simulations of mesogenic molecules were first performed some 15 years ago, relatively little progress has been made since that time in terms of using such simulations to inform mesogenic phase behaviour. This appears somewhat surprising, given the conclusion drawn from Wilson and Allen's (1991) early simulations on all-atom systems, that 1 ns is sufficient for establishing nematic order. However, as evidenced in the more recent review (Wilson 1999), this time-scale has proved to be a serious underestimate. Indeed, a recent (and impressive) foray by the Bologna group into all-atom modelling of aminocinnamate systems, which employed run-lengths of over 50 ns, concluded that order parameter stability could only be considered reliable when no significant drift was observed for 10 ns (Berardi *et al* 2004). Sadly, this casts doubt on the thermodynamic stability of many of the previous all-atom simulations of bulk LC behaviour.

In addition to this considerable issue of the time-scales required for establishing nematic stability in all-atom models, recent evidence suggests that a non-trivial system-size threshold also needs to be exceeded before a qualitative temperature dependence of orientational observables (particularly the nematic order parameter) can be achieved. Thus, while Berardi *et al* (2004) were able to establish nematic stability in their very long runs, they failed to observe increasing nematic order with decrease in temperature in their simulations of 98-molecule systems. However, increasing system size to hundreds of molecules (i.e. thousands of atomic interaction sites) *has* been shown by recent studies, e.g. (McDonald and Hanna 2004, Cheung *et al* 2004), to yield a qualitatively correct temperature dependence of the order parameter. Even here, though, a long-lived dependence on the choice of initial conditions can prove significant (McDonald 2002). Now that these issues are recognized, it is to be hoped that more progress will start to be made in this field through application of parallel MD approaches along with, e.g. multiple timestep methods and efficient treatments of long range interactions (Glaser 2000).

Due to the uncertainties associated with the simulations performed to date with all-atom models, it is not appropriate to draw too many conclusions regarding the various model parametrizations employed. In the main, these have been based on parameter sets derived for liquid-state simulation (e.g. Amber), both with and without various electrostatic contributions.

For the cyanobiphenyl family, for example, numerous alternative models have been derived (Picken *et al* 1989, Cross and Fung 1994, Cleaver and Tildesley 1994, Yoneya and Iwakabe 1995, Clark *et al* 1997, Lansac *et al* 2001, Cacelli *et al* 2002), through various combinations of standard force fields and explicit quantum chemical calculation. Despite this wealth of models, however, the computational difficulties raised above have conspired to prevent any thorough comparative studies from being performed. Thus, even for these much-studied cyanobiphenyl systems, there is no clear consensus as to which intramolecular components (e.g. detailed torsional potentials, partial charges, point dipoles and quadrupoles) are required for an all-atom model to successfully achieve quantitative agreement with experimental observations.

Notwithstanding these limitations in terms of phase behaviour, some noteworthy achievements have been made using all-atom models to investigate intramolecular structure (Wilson 1999, Berardi *et al* 2004), Kirkwood correlation factors (Cook and Wilson 2000) and the local structure of preconstructed smectic arrangements (Lansac *et al* 2001). Also, methodologies for the calculation of larger length-scale properties, such as the rotational viscosity (Cheung *et al* 2002) and flexoelectric coefficients (Cheung *et al* 2004), have now been applied to some all-atom systems.

3.3. Generic models—their bases, uses and limitations

The use of generic LC models is founded on the notion that much can be learned about mesogenic behaviour without recourse to intimate molecular detail. This view is supported by theory, most obviously Onsager's classic proof that shape anisotropy alone can be sufficient to induce nematic order (Onsager 1949). Also experimental work on a diverse range of systems (e.g. suspensions of tobacco mosaic virus, cylindical micelles, chromonic stacks and latex ellipsoids) has shown that LC order is exhibited by a range of non-molecular bodies with high shape anisotropies. Thus, the relatively slow rate of progress in all-atom simulations of LC systems has run in parallel with (and, arguably, motivated) the development and use of a series of simplified (or 'generic') models which *do* offer routes for the systematic investigation of explicit relationships between underlying model properties and bulk behaviour. Furthermore, many of these models have proved amenable to treatment by various analytical approaches (such as density functional and integral equation theories), so that direct comparison of simulation and theoretical results has become an increasingly common approach in the development of this field.

3.3.1. Lattice models. The simplest generic model of LC behaviour is the lattice-based Lebwohl–Lasher model (Lebwohl and Lasher 1972, 1973). In this, unit vector spins, sited at the vertices of a simple cubic lattice, are free to rotate about their centres of mass, subject to interactions with their nearest neighbours. In its basic form, this interaction is the purely anisotropic, headless Maier–Saupe potential, originally developed for use in molecular field theory (Maier and Saupe 1958, 1959, 1960). The Lebwohl–Lasher model ignores the particulate basis of LC ordering, coarse-graining, instead, to the level where each of the interacting spins should probably be considered as a volume element containing a locally-ordered cluster of molecules (Berggren *et al* 2003). That said, other elements of its behaviour (e.g. the decay length of spin–spin orientational correlations (Fabbri and Zannoni 1986)) imply that the lattice spacing distance should be of the same order as a molecular length. Interestingly, Onsager's description of the N–I transition, in which the orientational entropy sacrificed on entering the nematic phase is balanced by enhanced translational entropy, is not applicable to Maier–Saupe-based approaches including the Lebwohl–Lasher and some related

off-lattice models, e.g. (Luckhurst and Romano 1981, Wei and Patey 1992b, De Luca *et al* 1994). In fact, results obtained using these latter models demonstrate the veracity of Born's (1916) original hypothesis that anisotropic dispersion interactions (allied with either no steric component or a spherically symmetric steric component) can also be sufficient to induce nematic order. Put another way, once such enthalpic free-energy contributions are introduced, the pure entropy-balancing Onsager picture can be subordinate to these additional terms.

Early work performed using the Lebwohl–Lasher model identified a temperature-driven onset of orientational order resembling the N–I transition (Zannoni 1979). This was confirmed by a comprehensive study by Fabbri and Zannoni (1986) who, as well as locating the transition, showed that this very simple model shows a pretransitional divergence of orientational correlations on cooling from the isotropic phase. Subsequently, Zhang *et al* (1992) employed histogram reweighting and finite-size-scaling techniques to confirm the transition to be weakly first order, and Cleaver and Allen (1991) examined the model's orientational elastic constants. A more structural perspective on the collective orientational ordering behaviour of this system is given in Gonin and Windle (1997).

The basic Lebwohl–Lasher model employs an orientation-dependent interaction potential with the same symmetry as the nematic phase (i.e. the second order Legendre polynomial). By introducing alternative additional terms, however, modified behaviour can be induced. Addition of a first order term, for example, giving the Kreiger–James model of ferromagnetism (Krieger and James 1954), allows the effect of local head–tail asymmetry to be assessed. Simulations of this model (Biscarini *et al* 1991) show, in agreement with mean field treatments, that this first order term can stabilize a low temperature ferroelectric nematic, a phase which has still defied clear experimental observation. Incorporation of a fourth rank term, alternatively, can be used to tune the shape of the order parameter–temperature curve (Romano 1994, Chiccoli *et al* 1997). Modifications of the original interaction term have also been used to incorporate additional anisotropy effects (Hashim and Romano 1999) and to investigate chiral (Memmer and Janssen 1998b, 1998a) and dimer (Luckhurst and Romano 1997) systems. A number of Lebwohl–Lasher model variants have also been used to simulate and investigate biaxial nematic behaviour (Luckhurst and Romano 1980, Biscarini *et al* 1995, Chiccoli *et al* 1999, Romano 2004a, 2004b).

This class system has also been used to investigate the properties of various two-component mixtures. The first work in this area studied the effects of low concentrations of fixed isotropic sites on the surrounding LC matrix (Hashim *et al* 1986). Subsequently, this model was developed to allow the isotropic sites to move around the system, and a wider range of relative concentrations was incorporated, allowing phase separation between isotropic and nematic regions (Hashim *et al* 1990). More recently, Bates (1998) has incorporated isotropic terms into the interaction scheme so as to give control over the interfacial properties of the phase separated systems, while Memmer and Janssen (1999) have studied the effects of chiral additives. All-mesogenic mixtures have also been studied. Hashim *et al* (1993) investigated the behaviour of rod-disc mixtures, particularly the balance between phase separation and biaxial phase formation. Also, Polson and Burnell (1997) performed an initial study of fractionation effects at the N–I transition of a binary calamitic mixture. These binary mixtures have now been thoroughly investigated by Yarmolenko (2003), who has also attempted some initial investigations of ternary systems.

3.3.2. Off-lattice generic models. We now consider the range of LC models in which freely-translating particles are used to represent individual molecules. The earliest work in this area concentrated on molecular shape alone and employed models of rigid, hard anisotropic particles. This approach was justified by both Onsager's proof that a purely steric systems can

exhibit a density-driven N–I transition (Onsager 1949), and simulation work on simple fluid systems which had shown that molecule shape plays the main role in determining structural properties. We concentrate here on identifying some of the key early papers in this hard particle work before listing some of the more recent diversifications in this field. Following this, we review the use of generic LC models incorporating both attractive and repulsive components.

Hard particle models. The earliest work on hard particle simulations of LCs was Veillard-Baron's investigation of the behaviour of hard ellipsoid systems (Vieillard-Baron 1972). While this work saw the development of some key algorithms and analysis techniques, the simulations themselves were restricted to short run-lengths. Thus, it was not until these systems were revisited by Frenkel and co-workers using Perram and Wertheim's formulation of the hard ellipsoid contact function (Perram *et al* 1984, Perram and Wertheim 1985) that their full phase behaviour became established. The first tentative phase diagram for three-dimensional hard ellipsoid systems, proposed by Frenkel *et al* (1981), contained four different phases, namely isotropic, nematic, plastic crystal and ordered crystal. A subsequent investigation by Frenkel and Mulder (1985) established the range of stability of these phases; specifically, calamitic nematic phases were found for particle elongations $k \geqslant 2.75$, the transition density reducing with increased molecular elongation. A decade later, following some dispute of these results, Allen and Mason (1995) performed a study of their system-size dependence which confirmed the validity of Frenkel and Mulder's phase diagram. An extension of this phase diagram was then produced by Camp *et al* (1996b), who located the N–I coexistence densities precisely using Gibbs–Duhem integration techniques. Studies by Allen (1990) and Camp and Allen (1997) of a biaxial version of the hard ellipsoid model then showed it to form isotropic, nematic and biaxial phases as well as confirming the discotic nematic behaviour originally found by Frenkel and Mulder (1985). Again, the N–I and discotic nematic–isotropic phase transitions were located using Gibbs–Duhem integration methods. The major conclusion to be drawn from these results is that the main prediction of Onsager's theory, made in the limit $k \to \infty$, continues to hold at the intermediate values $k \gtrsim 3$ that correspond to the elongations of common molecular mesogens.

Another much-used steric model for calamitic LC behaviour is the hard spherocylinder (i.e. a cylinder of length L and diameter D fitted with two hemispherical end-caps, so that $k = 1 + L/D$). This model is popular because its contact function, while still not given by a closed analytical expression, is more straightforward to calculate than that of the hard ellipsoid. This gives obvious computational advantages and makes comparison with theory more amenable—the hard spherocylinder was the model used by Onsager. Additionally, the spherocylinder resembles the shape of various colloidal mesogenic materials such as the tobacco mosaic virus (Zasadzinski and Meyer 1986, Dogic and Fraden 1997). There is no unique discotic equivalent of the hard spherocylinder; both cut-spheres (Veerman and Frenkel 1992) and short cylindrical segments (Bates and Frenkel 1998a) have been studied, however.

The first computer simulation on hard spherocylinders was again performed by Vieillard-Baron (1974) using elongations $k = 2$ and 3. This study did not find any LC phases since, as was shown subsequently, these are only stable for $k \geqslant 4.1$; Vieillard-Baron did attempt to investigate a system with $k = 6$ (for which the nematic phase *is* stable) but was thwarted by the lack of computational resources available to him. Over a decade later, Stroobants *et al* (1986) found that systems of perfectly parallel spherocylinders form a smectic A phase between the nematic liquid and crystalline solid. Subsequently, Veerman and Frenkel (1990) revisited Vieillard-Baron's hard spherocylinder systems with full orientational freedom; studying particles with elongations $k \in [0 : 6]$; these authors found isotropic, nematic and smectic A fluid phases. A more complete phase diagram was later proposed

by McGrother *et al* (1996b) which showed that as k was increased, the smectic A phase was stable for $k \geqslant 4.2$, whereas the nematic phase required $k \sim 5$. Bolhuis and Frenkel (1997) later refined this phase diagram and extended it up to the Onsager limit. From these studies the phase stability of the hard spherocylinder was established as:

- nematic: $k = 1 + \dfrac{L}{D} \geqslant 4.7$,
- smectic A: $k = 1 + \dfrac{L}{D} \geqslant 4.1$.

In addition to these hard ellipsoid and spherocylinder systems, a number of other hard particle mesogens have been studied. One of the simplest of these, a rigid linear hard sphere chain (Whittle and Masters 1991), proved to be one of the most problematic: here, because of their non-convex shapes, the molecules proved poor at sliding past one another, leading to the development of metastable glassy states in the vicinity of the N–I transition. The tendency of these systems to become irretrievably interlocked was overcome by Williamson and Jackson (1998) through the use of reptation moves. Once orientationally ordered, this model proved to be reasonably well behaved, exhibiting a stable nematic region and undergoing a reversible nematic–smectic A transition. The related rattling-hard-sphere-chain model studied by Wilson and Allen (1993) proved immune to this glassy behaviour at the N–I transition, and gave an effective route by which to study the effect of molecular rigidity on phase properties. Models comprising sphere chains with rigid (linear) and flexible subunits (McBride and Vega 2002) were subsequently used to study the use of partial molecular flexibility to tune in and out various smectic phases. The use of flexible end-chains to enhance smectic phase stability had previously been established by van Duijneveldt and Allen (1997) using hard spherocylinders with simple four-point-site chains at each end.

In recent years, the hard Gaussian overlap (HGO) model, which is based on the shape parameter of the Gay–Berne model (see below), has attracted renewed interest. The mesogenic properties of this model were first simulated by Padilla and Velasco (1997), who identified an N–I transition. For moderate elongations, the HGO model is a good approximation to the hard ellipsoid contact function in that the virial coefficients (and thus the equations of state, at least at low to moderate densities) of the two models are very similar (Bhethanabotla and Steele 1987). However, this is not the case for highly non-spherical particles (Rigby 1989, Huang and Bhethanabotla 1999), for which the behaviour of the two models differs appreciably. To assess this explicitly, de Miguel and Martín del Río have performed a direct comparison of the two models (de Miguel and Martín del Río 2001, 2003), and found their behaviours to be equivalent qualitatively but not quantitatively; for each given particle elongation $k \in [3 : 10]$ the equations of state are consistently shifted with respect to one another due to the larger average excluded volume of the HGO interaction.

The HGO model has the considerable advantage over the hard ellipsoid that its contact function takes a relatively simple closed form. As well as making simulations easier to perform, this closed form allows the excluded volume of a pair of HGO particles to be calculated analytically (Velasco and Mederos 1998), so making direct comparison possible with second virial-based theories. The HGO shape parameter can also be extended and generalized, allowing for a variety of particle shapes and mixtures thereof to be simulated very efficiently. Since the majority of these generalizations have been employed in Gay–Berne-like 12-6 potentials, we defer a full listing to the following subsection. Here, we simply pick out the study by Barmes *et al* (2003) of hard tapered or pear-shaped objects performed using of one of these generalized HGO models. Here, both nematic and bilayer smectic phases have been found, the latter remaining stable for axial ratios as low as $k = 3.0$, i.e. significantly lower than the $k = 4.1$ required for hard spherocylinders to form a

smectic. Hard particle models of bent-core systems, related to the banana-shaped molecules more recently found to yield biaxial nematic behaviour (Acharya *et al* 2004, Madsen *et al* 2004), have also been investigated. These studies, based on spherocylinder dimer models, have found isotropic, nematic and both para electric and antiferro-electic smectic A phases (Camp *et al* 1996a, Lansac *et al* 2003). The extension of this class of model to spherocylinder trimers arranged in a zig-zag shape has led to the observation of remarkably rich phase behaviour for a purely steric model: depending on the zig-zag angle, this model gives columnar, smectic A or tilted smectic arrangements when expanded from a crystalline state (Maiti *et al* 1958).

Hard particle models have also been used to investigate various mixture systems. For example, in systems of length bi-disperse parallel spherocylinders, Stroobants (1992) found that, at high densitites, the smectic phase becomes unstable with respect to columnar order. Similar behaviour was observed in a subsequent study of polydisperse rods (Bates and Frenkel 1998b), although here the destabilization of the smectic phase did not occur until the level of polydispersity was moderately high. Rod–disc mixtures of hard particles with conjugate asymmetries (i.e. elongations k and $1/k$) have been used to investigate the balance, at near equimolar concentrations, between biaxiality and phase separation (Camp and Allen 1996, Camp *et al* 1997), the latter being the only finding in an independent study of a similar system (Galindo *et al* 2000). Also, mixtures of spheres and parallel spherocylinders have been shown to form a microphase separated lamellar phase (Koda *et al* 1996, Dogic *et al* 2000), whereas mixtures of hard spheres and freely rotating HGO ellipsoids can exhibit full phase separation at the N–I transition (Antypov and Cleaver 2003).

Before closing this subsection, we note another class of purely-repulsive model mesogen that has attracted some interest. These 'soft repulsive' systems, are all based, qualitatively at least, on the Weeks–Chandler–Anderson truncation of the Lennard-Jones potential (Weeks *et al* 1971). Since the repulsions in these systems are finite, temperature becomes a significant thermodynamic variable. The extra complication associated with this increase in phase space is largely offset, however, by certain pragmatic advantages; due to their smoothly varying interactions, these systems are both well-suited to conventional (readily parallelizable) MD approaches and less prone to structural bottlenecks than their hard particle equivalents. Furthermore, the intrinsically short range of their interactions makes them computationally efficient. While the results obtained for linear soft sphere chains (Paolini *et al* 1993) and soft repulsive spherocylinders (Earl *et al* 2001) are qualitatively indistinguishable from those of their hard particle equivalents, Xu *et al* (1999) have used an innovative bent-rod soft-sphere system to investigate onset of tilted smectic behaviour. Also, Andrienko *et al* (2001) have exploited the highly efficient soft Gaussian overlap model (which was actually first used by Kushick and Berne (1973)) to simulate the necessarily large volume of mesogenic solvent needed to examine the defect structures associated with various LC colloid systems—this type of model is, then, a good candidate for exploration of structural behaviours on length-scales up to 1 μm.

Soft particle models. As well as this work on hard particle modelling of LCs, a further series of generic models have been developed which incorporate attractive particle–particle interactions. Applications involving this class of model are dominated by variants of the Gay–Berne model (Gay and Berne 1981), a single-site model in which the particle shape and interaction well depth can both be made anisotropic. The Gay–Berne model has arguably been the most successful and popular model for LC simulation to date; however, it also has a significant number of detractors. For this reason, we start this subsection by giving both a description of its basis and a critique of its limitations.

The standard Gay–Berne model has, at its core, Berne and Pechukas' HGO shape parameter (Berne and Pechukas 1972),

$$\sigma(\hat{\mathbf{r}}_{ij}, \hat{\mathbf{u}}_i, \hat{\mathbf{u}}_j) = \sigma_0 \left[1 - \frac{\chi}{2} \left\{ \frac{(\hat{\mathbf{r}}_{ij} \cdot \hat{\mathbf{u}}_i + \hat{\mathbf{r}}_{ij} \cdot \hat{\mathbf{u}}_j)^2}{1 + \chi(\hat{\mathbf{u}}_i \cdot \hat{\mathbf{u}}_j)} + \frac{(\hat{\mathbf{r}}_{ij} \cdot \hat{\mathbf{u}}_i - \hat{\mathbf{r}}_{ij} \cdot \hat{\mathbf{u}}_j)^2}{1 - \chi(\hat{\mathbf{u}}_i \cdot \hat{\mathbf{u}}_j)} \right\} \right]^{-1/2}, \tag{1}$$

where $\hat{\mathbf{r}}_{ij} = \mathbf{r}_{ij}/r_{ij}$ is a unit vector along the vector $\mathbf{r}_{ij} = \mathbf{r}_i - \mathbf{r}_j$ between particles i and j and the unit vectors $\hat{\mathbf{u}}_i$ and $\hat{\mathbf{u}}_j$ denote their orientations. Here, χ is a fully specified function of the particle length to breadth ratio, l/d, and is given by

$$\chi = \frac{(l/d)^2 - 1}{(l/d)^2 + 1}. \tag{2}$$

As is apparent from these expressions, in this original version of the model, particles i and j are assumed to have both axial and head–tail symmetry. Simplified and generalized versions of equation (1) have been determined for the cases where, respectively, one of the particles is a small (Berne and Pechukas 1972) or large (Antypov and Cleaver 2004a) sphere or the axis lengths of particles i and j are different from one another (Cleaver *et al* 1996). The utility of these generalizations is that they give the shape parameter in a relatively simple closed analytical form. This makes them straightforward to implement in MD or MC simulation or in, e.g. density functional or integral equation theories. More complex routes to the Gaussian overlap shape parameter, based on on-the-fly matrix inversions, have been proposed and implemented for biaxial particles (Ayton and Patey 1995, Berardi *et al* 1998, Berardi and Zannoni 2000). Gaussian overlap shape parameters, based on expansions of Stone functions (Stone 1978), have also been proposed (Zewdie 1998b) for the generation of alternative particle shapes. This expansion approach has been used to simulate tapered, or pear-shaped, particles (Berardi *et al* 2001), and it appears a viable, if complex, route for the generation of lower-symmetry objects. For cylindrically symmetric objects, a parametric generalization of equation (1) developed by Barmes *et al* (2003) is a computationally efficient variant of Zewdie's expansion approach. Furthermore, being based on the HGO mixture formalism of Cleaver *et al* (1996), this parametric approach offers a natural route to the study of more exotic multi-component mixtures (e.g. pear shaped objects mixed with polydisperse rods).

Equation (1) reveals both the utility and the foibles of the Gay–Berne class of model: it gives the effective contact distance between particles i and j in a form which is analytically closed but which cannot be expressed as a simple sum of contributions from each of the two particles. Indeed, due to its Gaussian overlap origins, the HGO contact distance is in fact non-additive (i.e. it does not satisfy the Lorentz–Bertholet mixing rule) and there is no formal definition of the single-particle volume. This apparent failing is, from a chemist's perspective, actually quite reasonable—due to their intramolecular flexibility, real mesogenic molecules do not have additive contact functions or fixed excluded volumes either. Furthermore, the qualitative equivalence of the mesogenic behaviours of Gay–Berne (or HGO-based) fluids and those of hard-ellipsoid-based potentials indicates that the approximations involved in the former are quite reasonable when all that is being sought is an understanding of generic phase behaviour. For situations where the ratio of the largest to the smallest particle semi-axis lengths grows too large, however, the issue of non-addivity becomes significant, and the fundamentals of the potential need to be addressed (see, e.g. Antypov and Cleaver (2004a), Barmes and Cleaver (2005)). Also, due to issues related to the orientation-dependent particle volume of Gaussian overlap models, difficulties can arise if Gay–Berne-like interaction sites are used in coarse-grained models of specific LC molecules.

When Kushick and Berne (1973) first employed the Berne and Pechukas shape parameter, equation (1), in a standard Lennard-Jones-like 12-6 interaction potential the resultant model

was found to suffer unrealistic features such as equal well-depths but unequal well-widths for end-to-end and side-by-side parallel molecular arrangements. These deficiencies were subsequently resolved by Gay and Berne (1981), who modified the functional form of the Berne–Pechukas potential so that it could give a reasonable fit to a linear arrangement of four Lennard-Jones sites. This resulted in the now widely used Gay–Berne potential, $\mathcal{V}^{\mathrm{GB}}$, expressed as

$$\mathcal{V}^{\mathrm{GB}} = 4\epsilon(\hat{\mathbf{u}}_i, \hat{\mathbf{u}}_j, \hat{\mathbf{r}}_{ij})\{R^{12} - R^6\} \tag{3}$$

with

$$R = \frac{\sigma_0}{r - \sigma(\hat{\mathbf{u}}_i, \hat{\mathbf{u}}_j, \hat{\mathbf{r}}_{ij}) + \sigma_0}.$$

Here, the strength parameter is defined as

$$\epsilon(\hat{\mathbf{u}}_i, \hat{\mathbf{u}}_j, \hat{\mathbf{r}}_{ij}) = \epsilon_0 \epsilon_1^{\nu}(\hat{\mathbf{u}}_i, \hat{\mathbf{u}}_j)\epsilon_2^{\mu}(\hat{\mathbf{u}}_j, \hat{\mathbf{u}}_j, \hat{\mathbf{r}}_{ij}) \tag{4}$$

with

$$\epsilon_1(\hat{\mathbf{u}}_i, \hat{\mathbf{u}}_j) = \left[1 - \chi^2(\hat{\mathbf{u}}_i \cdot \hat{\mathbf{u}}_j)^2\right]^{-1/2} \tag{5}$$

and

$$\epsilon_2(\hat{\mathbf{u}}_i, \hat{\mathbf{u}}_j, \hat{\mathbf{r}}_{ij}) = 1 - \frac{1}{2}\chi'\left[\frac{(\hat{\mathbf{r}}_{ij} \cdot \hat{\mathbf{u}}_i + \hat{\mathbf{r}}_{ij} \cdot \hat{\mathbf{u}}_j)^2}{1 + \chi'(\hat{\mathbf{u}}_i \cdot \hat{\mathbf{u}}_j)} + \frac{(\hat{\mathbf{r}}_{ij} \cdot \hat{\mathbf{u}}_i - \hat{\mathbf{r}}_{ij} \cdot \hat{\mathbf{u}}_j)^2}{1 - \chi'(\hat{\mathbf{u}}_i \cdot \hat{\mathbf{u}}_j)}\right]. \tag{6}$$

χ' is the energy anisotropy parameter defined using k', the ratio of end-to-end and side-by-side well depths (ϵ_{ee} and ϵ_{ss}, respectively). Thus,

$$\begin{aligned} \chi' &= \frac{k'^{\mu^{-1}} - 1}{k'^{\mu^{-1}} + 1}, \\ k' &= \frac{\epsilon_{\mathrm{ee}}}{\epsilon_{\mathrm{ss}}}. \end{aligned} \tag{7}$$

The behaviour of the Gay–Berne model can be tuned through modification of the four parameters k, k', μ and ν. The most studied parametrization, $\mathrm{GB}(k, k', \nu, \mu) = \mathrm{GB}(3, 5^{-1}, 1, 2)$, is that put forward by Gay and Berne (1981) from their fits to linear arrays of Lennard-Jones sites. Preliminary simulations performed by Adams *et al* (1987) using this parametrization showed the model to be suitable for LC modelling and found both isotropic and nematic phases. Subsequently, Luckhurst *et al* (1990), using the slightly different parametrization $\mathrm{GB}(3, 5^{-1}, 2, 1)$, found much richer phase behaviour comprising isotropic, nematic, smectic A, smectic B and crystal phases. Independent of this, a thorough study of the original $\mathrm{GB}(3, 5^{-1}, 1, 2)$ parametrization by the Seville group identified its liquid–vapour coexistence envelope (de Miguel *et al* 1990) and showed that its fluid phase diagram also contains a region of smectic A stability (deMiguel *et al* 1991a, 1991b, Chalam 1991, deMiguel 1993). The parametrization $\mathrm{GB}(3, 5^{-1}, 3, 1)$ was used by other groups (Berardi *et al* 1993, Allen *et al* 1996b); while this gives the same isotropic, nematic and smectic phases as the previous parametrizations, the increased value of μ allows for a wider window of nematic stability. The substantially different parametrization $\mathrm{GB}(4.4, 39.6^{-1}, 0.74, 0.8)$ was introduced by Luckhurst and Simmonds (1993) in an attempt to use a model more closely related to real molecular mesogens. This parametrization was obtained from fitting the Gay–Berne potential to an axial average of an all-atom representation of the *p*-terphenyl molecule. Subsequently, Bates and Luckhurst (1999) performed a thorough study using the parametrization $\mathrm{GB}(4.4, 20^{-1}, 1, 1)$ and found the model to exhibit isotropic, nematic, smectic A and smectic B phases in good agreement with the behaviour of such real mesogens.

An investigation into the generic effects of the attractive part of the potential (de Miguel *et al* 1996) showed the importance of attractive forces for the formation of smectic phases by ellipsoidal particles, layered phases being favoured by an increase in $1/k'$. A related study into the effects of molecular elongation, k, on the Gay–Berne phase diagram (Brown *et al* 1998) showed significant changes, notably in the liquid–vapour coexistence region.

The Gay–Berne potential can also be readily modified to yield discotic behaviour. De Luca *et al* (1994) used the anisotropic Gay–Berne well-depth term with a spherical core to obtain a discotic nematic phase, whereas Emerson *et al* (1994) used the full Gay–Berne interaction with $k = 0.345$ to observe both discotic nematic and columnar phases. Here, the arrangement of the discotic columns was found to depend on the level of interdigitation required at different densities. Subsequently, Bates and Luckhurst (1998) performed a more extensive investigation of this class of system, using a slightly modified version of equation (3), and a similar system was revisited by Zewdie (1998a) as an application of his expansion-function approach to the shape parameter.

One of the most insightful recent findings from LC simulation has been Berardi and Zannoni (2000) discovery of a biaxial nematic phase arising from a combination of steric and dispersive interactions. Here, using Gay–Berne particles with moderate shape biaxiality, a biaxial nematic phase was successfully stabilized by enhancing attractions between the particle edges (rather than their faces). Other departures from uniaxial molecule shapes largely have their origins in Neal *et al*'s (1997) use of three-Gay–Berne-site assemblies to investigate triangular and zig-zag shaped mesogens. The former were subsequently simplified to Gay–Berne plus sphere models of pear-shaped particles (Stelzer *et al* 1999, Billeter and pelcovits 2000) with measurable flexoelectric coefficients. Following this, tapered variants of single-site Gay–Berne particles with appropriately tuned dispersive interactions were refined to the point where they yielded a ferroelectric nematic phase (Berardi *et al* 2001, 2004), behaviour which, at the time of writing, has yet to be achieved experimentally. Neal *et al*'s (1997) zig-zag model, meanwhile, inspired a single-site mimic comprising Gay–Berne shape and well-depth functions aligned along separate axes (Withers *et al* 2000). This internally rotated Gay–Berne model readily yielded tilted smectic phases on cooling from isotropic configurations. More recently, multi-site models have been developed for bent-core molecules. These include two-site Gay–Berne models (Memmer 2000b, Johnston *et al* 2002) and seven-site bi-linear arrays of Lennard-Jones sites (Dewar and Camp 2004). In the latter case, a tilted smectic phase has been observed for small and moderate core–core angles, but this may be associated with the preference of sphere chains to adopt staggered packing arrangements. The link between molecular and phase chirality has been investigated using generic models in a number of papers by Memmer (Memmer *et al* 1993, Memmer 2000a, 2001). Using an alternative, less prescriptive, approach to the imposition of boundary conditions on such systems, Varga and Jackson (2003) have observed chiral pitch values much greater than the sample dimensions.

Simulations of bidisperse mixtures of calamitic Gay–Berne molecules have confirmed experimental findings that, even in well-mixed systems, more mesogenic particles have higher order parameters than their less mesogenic counterparts (Bemrose *et al* 1997). Through Gibbs ensemble Monte Carlo simulations of such systems, Mills and Cleaver (2000) have also made direct measurements of compositional fractionation of LC mixtures at the N–I transition. This finding is related to the behaviour observed in simulations of associating LCs (McGrother *et al* 1997, Berardi *et al* 1999). Here, short particles, able to dimerize via attractive end-sites, exhibit strong increases in dimerization with the onset of nematic order. The prospect of even more exotic associating behaviour has been raised by the range of structures observed in recent simulations of rod–sphere mixtures (Antypov and Cleaver 2004b).

Finally, in this subsection, we note that a considerable body of work has been amassed investigating the effect of electrostatic dipole and quadrupole moments on mesogenic behaviour. In virtually all cases, such studies have involved incorporation of these electrostatic contributions into established generic hard and soft particle models. As noted by (McGrother *et al* 1998), however, the effects of dipoles, in particular, have proved to be strongly dependent on the details of their location and orientation on the host particles.

Some of the earliest studies of this class of system revealed that dipolar hard- and soft-spheres can exhibit ferroelectric nematic behaviour (Weis *et al* 1992, Wei and Patey 1992a, 1992b); however, the stability of these monodomains was later found to be dependent on the nature of the far-field electrostatic boundary conditions (Banerjee *et al* 1998). In a follow-up simulation study (Ayton and Patey 1996, Ayton *et al* 1997), polar fluid behaviour was found to persist only for weakly discotic particle shapes. Similarly, no ferroelectric nematic behaviour has been observed in any of the uniaxial-calamitic-particle plus dipole models that have been studied. Extensive simulations by Jackson and co-workers on dipolar hard spherocylinder systems with central longitudinal dipoles (McGrother *et al* 1996a, 1998, Gil-Villegas *et al* 1997a) found the nematic phase to be destabilized with respect to both isotropic and smectic A phases, disappearing altogether at low temperatures. For terminal longitudinal dipoles, however, the range of nematic phase stability was found to be increased (McGrother *et al* 1996a). For central transverse dipoles, enhanced stability of the smectic A phase was again observed, with the additional feature of some in-plane chain- and ring-formation by the transverse dipoles (Gil-Villegas *et al* 1997b). Similar studies performed on dipolar Gay–Berne systems have drawn largely equivalent conclusions. Thus, for Gay–Berne systems with central longitudinal dipoles (Satoh *et al* 1996a, Houssa *et al* 1998, 1999), enhanced smectic phase stability was observed, whereas the nematic was favoured on shifting the dipole to a terminal location (Satoh *et al* 1996b). For some parametrizations of the latter system, the smectic phase was found to develop a bilayer structure (Berardi *et al* 1996b, 1996a). Central transverse dipoles were found to have little effect on the mesogenic behaviour of Gay–Berne systems (Gwóźdź *et al* 1997). However, multiple electrostatic moments *have* been shown to have significant effects. Specifically, by studying two outboard dipoles at various angles to the molecular axis, Berardi *et al* (2003) determined systems able to form tilted smectic phases. Tilted smectic behaviour had previously been induced in Gay–Berne systems through the inclusion of longitudinal point quadrupole moments (Neal and Parker 1998, Withers *et al* 2002, Withers 2003). For transverse central quadrupoles, conversely, Neal and Parker (2000) observed a significant increase in T_{NI}, even for small quadrupole moments. At larger quadrupole values, this study also observed cubic smectic arrangements rather than the usual smectic B behaviour.

4. Mesoscopic simulations

Although molecular simulation methods are becoming increasingly successful at predicting the behaviour of LC materials on microscopic scales, for many applications it is also important to be able to model their behaviour at much longer length- and time-scales. For example, simulations at length-scales greater than 1 μm and time-scales greater than 1 ms will be required to model a display device. These length- and time-scales are inaccessible to molecular simulations, and it is therefore necessary to employ either macroscopic or mesoscopic methods. The equations governing the dynamics of a nematic with fixed order parameter are well established; if the material parameters are well defined, either by experiment or molecular simulation, and the system being considered is relatively simple, analytical or standard numerical solutions of the macroscopic equations may be the most appropriate way of determining the behaviour of

the material at long length- and time-scales (e.g. Leslie (1979), Stewart (2003)). Finite element methods have also been used to determine the response of an LC system at the macroscale (e.g. Yoon *et al* (2004), James *et al* (2004)). For nematics with a variable order parameter there are, as explained below, a number of choices for the governing equations; once again, these may be solved by standard numerical methods (e.g. Svensek and Zumer (2002)). However, such methods are not always appropriate. Thus, for example, close to interfaces they are normally unable to model correctly systems with weak anchoring.

In order to model more complex systems such as confined LCs or mixtures of LCs with isotropic fluids, an alternative approach is to use a mesoscopic simulation method, such as the LB method. Such methods have the potential benefit that the underlying physics can be built into the rules of the simulation method and the macroscopic behaviour is then emergent. In addition to providing an efficient simulation scheme, the approach has the merit of providing insight into the origin of the macroscopic behaviour and may also provide a route to bridging the length-scales from the microscopic to macroscopic. However, a successful paradigm for bridging from molecular to macroscopic length-scales has yet to be developed.

There are a variety of mesoscopic simulation methods available for modelling fluids. These include, for example, dissipative particle dynamics (DPD) (e.g. Hoogerbrugge and Koelman (1992), Pagonabarraga and Frenkel (2001), Espanol and Revenga (2003)), smoothed particle dynamics (e.g. Monaghan (1992), Kum *et al* (1995)) and the LB method (e.g. Succi (2001)). The LB method is essentially the only mesoscopic technique which has been developed in any detail to model LCs and the remainder of this section is devoted to the method. A number of LB schemes have been developed to represent the flow of nematic LCs (Care *et al* 2000, 2003, Denniston *et al* 2001a, 2004, Spencer and Care 2005) and in the remainder of this section we review these methods and their applications. As far as the authors are aware, no attempt has been made to develop LB methods for any other LC mesophases. We should mention in passing that the LB method is able to model other phases of complex fluids; for example, LB models of amphiphilic systems have been able to to recover the gyroid phase (Gonzalez-Segredo and Coveney 2004). We note that Levine *et al* (2005) have recently reported the use of DPD to model nematic and smectic phases; however, the approach they use is closer to the molecular simulations reported in section 3 than the mesoscale approach which is the focus of this section.

We begin by reviewing the various macroscopic formalisms which have been employed as the target for the LB schemes. Rather than impose a single unified notation, we have adopted in each section the notation used in the appropriate literature. Although this has the consequence that the same physical quantity is sometimes described by different symbols, the reader should find the transition to the literature is achieved more readily.

4.1. Macroscopic equations for nemato-dynamics

The first choice which must be made in modelling a nematic LC is whether the order parameter can be considered to be essentially constant. For many systems this is a reasonable approximation and the Ericksen–Leslie–Parodi formalism (e.g. deGennes and Prost (1993), Chandrasekhar (1992), Stewart (2003)) is a commonly used series of equations for such systems. Care *et al* (2000) developed an LB method based on the ELP equations.

However, in many systems the spatial and temporal variation of the order parameter is important; for example, in the presence of defects, close to substrates or in shear-flows when the LC is close to the nematic–isotropic transition temperature. If the order parameter is allowed to vary, there are a number of different presentations of nemato-dynamics, with perhaps the earliest work by Hess (1975). A recent paper by Sonnet *et al* (2004) using arguments based

on Rayleigh's dissipation function (e.g. Vertogen and de Jeu (1988)) provides the basis upon which the variety of schemes with a variable order parameter may be compared.

The variable order parameter schemes are more straightforward to adapt to an LB formalism and the two approaches which have been used as the basis of LB nemato-dynamics are due to Qian and Sheng (1998) and Beris and Edwards (1994). The latter work is closely related to that of Olmsted and Goldbart (1990), which was also influenced by the work of Doi (1981) and Kuzuu and Doi (1983) on polymer rheology.

4.1.1. Constant order parameter: Ericksen–Leslie–Parodi formalism. If the order parameter is assumed to be constant throughout the system, the most usual form of the macroscopic equations are the Ericksen–Leslie–Parodi (ELP) equations of nemato-dynamics for an incompressible fluid, although there is an alternative 'Harvard' formalism (deGennes and Prost 1993). These equations may be summarized as follows:

$$\nabla_\alpha v_\alpha = 0, \tag{8}$$

$$\frac{\mathrm{D}v_\beta}{\mathrm{D}t} = \partial_\alpha \sigma_{\alpha\beta}, \tag{9}$$

$$h_\alpha = \gamma_1 N_\alpha + \gamma_2 n_\beta A_{\beta\alpha}, \tag{10}$$

where

$$N_\alpha = \frac{\mathrm{D}n_\alpha}{\mathrm{D}t} - \varepsilon_{\alpha\beta\gamma}\omega_\beta n_\gamma. \tag{11}$$

The first two equations are the equations of continuity (8) and momentum evolution (9). Equation (10) may be considered to be an equation controlling the evolution of the director, n_α. In these equations, we use the repeated index summation convention for summation over Cartesian indices, $\mathrm{D}/\mathrm{D}t$ is the convective derivative, $\sigma_{\alpha\beta}$ is the stress tensor, $A_{\alpha\beta} = 1/2(\partial_\alpha v_\beta + \partial_\beta v_\alpha)$ is the symmetric part of the velocity gradient tensor and $\omega_\alpha = (1/2)\varepsilon_{\alpha\beta\gamma}\partial_\beta v_\gamma$ is the fluid vorticity. The field $h_\alpha(\mathbf{x}, t)$ is a 'molecular field' which mediates the effects of (i) the Frank elastic energy and (ii) the effect of any external applied magnetic or electric fields. In the one-constant approximation, in which the three Frank elastic constants are assumed to be equal to a single constant, K, the molecular field becomes

$$h_\alpha = K\partial_\beta\partial_\beta n_\alpha + \chi_a(\mathbf{H}.\mathbf{n})H_\alpha, \tag{12}$$

where, for example, H_α is the external magnetic field and χ_a is the anisotropy in the susceptibility. The viscous part of the stress tensor for a nematic may be written in the form

$$\sigma'_{\alpha\beta} = (\alpha_2 n_\alpha h_\beta + \alpha_3 h_\alpha n_\beta)/\gamma_1 + \alpha_1 n_\alpha n_\beta n_\gamma n_\delta A_{\gamma\delta} + \alpha_4 A_{\alpha\beta},$$
$$(\alpha_5 - \alpha_2\gamma_2/\gamma_1)n_\alpha n_\gamma A_{\gamma\beta} + (\alpha_6 - \alpha_3\gamma_2/\gamma_1)n_\beta n_\gamma A_{\gamma\alpha}, \tag{13}$$

where

$$\gamma_1 = \alpha_3 - \alpha_2, \tag{14}$$

$$\gamma_2 = \alpha_6 - \alpha_5 = \alpha_2 + \alpha_3. \tag{15}$$

The latter relationship due to Parodi embodies Onsager's reciprocal relations for irreversible processes (e.g. Chandrasekhar (1992)).

4.1.2. Variable order parameter: Beris–Edwards formalism. If the order parameter cannot be assumed to be a constant, the formalism of nemato-dynamics is normally written in terms

of evolution equations for the pressure, velocity and a tensor order parameter, $Q_{\alpha\beta}$. This latter quantity may be written as

$$Q_{\alpha\beta} = \langle m_\alpha m_\beta - \tfrac{1}{3}\delta_{\alpha\beta}\rangle, \tag{16}$$

where m_α is a unit vector defining the orientation of an individual molecule and $\langle\ \rangle$ denotes an average over all the molecules in the system. For a nematic with uniaxial symmetry,

$$Q_{\alpha\beta} = S(n_\alpha n_\beta - \tfrac{1}{3}\delta_{\alpha\beta}). \tag{17}$$

However, in general it must be assumed that the system will exhibit biaxiality; this is particularly important close to walls or defects.

In this section we present the equations of Beris and Edwards' (1994) formalism and essentially follow the notation adopted by Denniston *et al* (2001a); in the subsequent section we present the Qian and Sheng (1998) formalism. It should be noted that the Beris–Edwards and Qian–Sheng equations reduce to the ELP formalism in the limit that the order parameter becomes independent of time and position. However, Sonnet *et al* (2004) show that the two schemes differ in the terms which are included in the dissipation function.

In the Beris–Edwards scheme, the evolution equation for $Q_{\alpha\beta}(\equiv \mathbf{Q})$ is

$$\frac{\mathrm{D}\mathbf{Q}}{\mathrm{D}t} - \mathbf{S}(\mathbf{W}, \mathbf{Q}) = \Gamma\mathbf{H}, \tag{18}$$

where Γ is a rotational diffusion constant. The first term on the left-hand side is the convective derivative for $\mathbf{Q}$ and the second term couples the velocity gradient tensor $W_{\alpha\beta} = \partial_\beta u_\alpha$ and the order tensor. To lowest order in $\mathbf{Q}$ this is given by

$$\mathbf{S}(\mathbf{W}, \mathbf{Q}) = (\xi\mathbf{A} + \boldsymbol{\Omega})\left(\mathbf{Q} + \frac{\mathbf{I}}{3}\right) + \left(\mathbf{Q} + \frac{\mathbf{I}}{3}\right)(\xi\mathbf{A} - \boldsymbol{\Omega}) - 2\xi\left(\mathbf{Q} + \frac{\mathbf{I}}{3}\right)\mathrm{Tr}(\mathbf{QW}), \tag{19}$$

where $\mathbf{A} = (\mathbf{W} + \mathbf{W}^T)/2$ is the symmetric, and $\boldsymbol{\Omega} = (\mathbf{W} - \mathbf{W}^T)/2$ is the antisymmetric, velocity gradient tensor. We note that $\boldsymbol{\Omega}$ is related to the vorticity through $\Omega_{\alpha\beta} = -\varepsilon_{\alpha\beta\gamma}\omega_\gamma$. The parameter ξ is a material parameter which depends upon the molecular properties of the LC. The function $\mathbf{S}$ arises because the flow fields can both rotate the director and modify the order parameter. The molecular field, $\mathbf{H}$, controls the relaxation to equilibrium and is derived from appropriate moments of the free energy, $\mathcal{F}$,

$$\mathbf{H} = -\frac{\delta\mathcal{F}}{\delta\mathbf{Q}} + \frac{\mathbf{I}}{3}\mathrm{Tr}\frac{\delta\mathcal{F}}{\delta\mathbf{Q}}. \tag{20}$$

If the free energy is given by

$$\mathcal{F} = \int \mathrm{d}^3 r \left\{\frac{a}{2}Q_{\alpha\beta}^2 - \frac{b}{3}Q_{\alpha\beta}Q_{\beta\gamma}Q_{\gamma\alpha} + \frac{c}{4}(Q_{\alpha\beta}^2)^2 + \frac{K}{2}(\partial_\alpha Q_{\beta\gamma})^2\right\}, \tag{21}$$

The first three terms are the standard Landau–deGennes free energy which controls the nematic–isotropic phase transition and the equilibrium of the nematic in the absence of gradients in the order parameter. The last term is the elastic free energy in the one-constant approximation. The molecular field derived from $\mathcal{F}$ is

$$\mathbf{H} = -a\mathbf{Q} + b\left(\mathbf{Q}^2 - \frac{\mathbf{I}}{3}\mathrm{Tr}\mathbf{Q}^2\right) - c\mathbf{Q}\mathrm{Tr}\mathbf{Q}^2 + K\nabla^2\mathbf{Q}. \tag{22}$$

The fluid momentum obeys the Navier–Stokes type equations (8) and (9) with the stress tensor, $\sigma_{\alpha\beta}$, composed of a symmetric component

$$\begin{aligned}\sigma_{\alpha\beta}^s = &-P\delta_{\alpha\beta} + \eta A_{\alpha\beta} - \xi H_{\alpha\gamma}\left(Q_{\gamma\beta} + \frac{1}{3}\delta_{\gamma\beta}\right) - \xi\left(Q_{\alpha\gamma} + \frac{1}{3}\delta_{\alpha\gamma}\right)H_{\gamma\beta} \\ &+ 2\xi\left(Q_{\alpha\beta} + \frac{1}{3}\delta_{\alpha\beta}\right)Q_{\gamma\varepsilon}H_{\gamma\varepsilon} - \partial_\beta Q_{\gamma\varepsilon}\frac{\delta\mathcal{F}}{\delta\partial_\alpha Q_{\gamma\varepsilon}},\end{aligned} \tag{23}$$

and an antisymmetric component

$$\sigma^a_{\alpha\beta} = Q_{\alpha\gamma}H_{\gamma\beta} - H_{\alpha\gamma}Q_{\gamma\beta}, \tag{24}$$

and the pressure is taken to be

$$P = \rho T - \frac{K}{2}(\nabla \mathbf{Q})^2. \tag{25}$$

In equation (23), η is the parameter equivalent to the isotropic viscosity, α_4, of the ELP theory.

4.1.3. Variable order parameter: Qian–Sheng formalism An alternative formalism for the flow of a nematic LC with a variable scalar order parameter is due to Qian and Sheng (1998). It is important to note that Qian and Sheng (1998) employ a slightly different definition of the order tensor to that defined in equation (16). Hence they essentially define

$$Q_{\alpha\beta} = \langle \tfrac{1}{2}(3m_\alpha m_\beta - \delta_{\alpha\beta})\rangle, \tag{26}$$

and for a nematic with uniaxial symmetry this gives

$$Q_{\alpha\beta} = \frac{S}{2}(3n_\alpha n_\beta - \delta_{\alpha\beta}). \tag{27}$$

The definitions given by equations (16) and (26) both give a traceless tensor, but the eigenvalues are not identical. The two governing equations of the Qian and Sheng scheme are the momentum evolution equation,

$$\rho D_t u_\beta = \partial_\alpha(-P\delta_{\alpha\beta} + \sigma^d_{\alpha\beta} + \sigma^f_{\alpha\beta} + \sigma^v_{\alpha\beta}), \tag{28}$$

and the order tensor evolution equation,

$$J\ddot{Q}_{\alpha\beta} = h^e_{\alpha\beta} + h^v_{\alpha\beta} - \lambda^N\delta_{\alpha\beta} - \varepsilon_{\alpha\beta\gamma}\lambda^N_\gamma, \tag{29}$$

where $h^e_{\alpha\beta}$ ($h^v_{\alpha\beta}$) is the elastic (viscous) molecular field. The quantities λ^N and λ^N_α are Lagrange multipliers which impose the constraints that the order tensor, $Q_{\alpha\beta}$, is symmetric and traceless.

Qian and Sheng (1998) show that in the limit of constant order parameter, the solutions of these equations are identical to those obtained from the standard Ericksen–Leslie–Parodi equations (deGennes and Prost 1993). In equations (28) and (29), $D_t = \partial_t + u_\mu\partial_\mu$ is the convective derivative and P is the pressure in the nematic phase. $\sigma^v_{\alpha\beta}$ is the viscous stress tensor,

$$\begin{aligned}\sigma^v_{\alpha\beta} = {} & \beta_1 Q_{\alpha\beta}\,Q_{\mu\nu}A_{\mu\nu} + \beta_4 A_{\alpha\beta} + \beta_5 Q_{\alpha\mu}A_{\mu\beta} + \beta_6 Q_{\beta\mu}A_{\mu\alpha} + \tfrac{1}{2}\mu_2 N_{\alpha\beta} - \mu_1 Q_{\alpha\mu}N_{\mu\beta} \\ & + \mu_1 Q_{\beta\mu}N_{\mu\alpha},\end{aligned} \tag{30}$$

where $N_{\alpha\beta}$ is the co-rotational derivative defined by $N_{\alpha\beta} = \partial_t Q_{\alpha\beta} + u_\mu\partial_\mu Q_{\alpha\beta} - \varepsilon_{\alpha\mu\nu}\omega_\mu Q_{\nu\beta} - \varepsilon_{\beta\mu\nu}\omega_\mu Q_{\nu\alpha}$, with ω_μ being the fluid vorticity. In equation (30), $\sigma^d_{\alpha\beta}$ is the distortion stress tensor,

$$\sigma^d_{\alpha\beta} = -\frac{\partial f^N}{\partial\,(Q_{\mu\nu,\,\alpha})}Q_{\mu\nu,\,\beta}, \tag{31}$$

where $Q_{\alpha\beta,\gamma} \equiv \partial_\gamma(Q_{\alpha\beta})$ and $\sigma^f_{\alpha\beta}$ is the stress tensor associated with an externally applied field. The bulk elastic molecular field is given by

$$h^e_{\alpha\beta} = -\frac{\partial f^N}{\partial Q_{\alpha\beta}} + \partial_\mu\frac{\partial f^N}{\partial\,(Q_{\alpha\beta,\,\mu})}, \tag{32}$$

where the free energy density of the bulk nematic, f^N, is given by a Landau–deGennes expression of the form

$$f^N = f^{Nh} + f^{Ng}, \tag{33}$$

where the homogeneous contribution, f^{Nh}, is given by

$$f^{Nh} = \tfrac{1}{2}(\alpha_F Q_{\mu\nu}^2 - \beta_F Q_{\mu\nu} Q_{\nu\tau} Q_{\tau\mu} + \gamma_F (Q_{\mu\nu}^2)^2) \tag{34}$$

and the gradient contribution, f^{Ng}, is given by

$$f^{Ng} = \tfrac{1}{2}(L_1 Q_{\mu\nu,\tau}^2 + L_2 Q_{\mu\nu,\nu} Q_{\mu\tau,\tau}). \tag{35}$$

Using this form of the free energy, the bulk molecular field, equation (32), is given by

$$h_{\alpha\beta}^e = L_1 \partial_\mu^2 Q_{\alpha\beta} + L_2 \partial_\beta \partial_\mu Q_{\alpha\mu} - \alpha_F Q_{\alpha\beta} + 3\beta_F Q_{\alpha\mu} Q_{\beta\mu} - 4\gamma_F Q_{\alpha\beta} Q_{\mu\nu}^2. \tag{36}$$

The expressions (32)–(36) are essentially equivalent to equations (20)–(22) for the Beris–Edwards scheme. However, the free energy (21) only recovers the one-constant approximation for the elastic constants, whereas that used by Qian–Sheng allows for two independent elastic constants defined in terms of L_1 and L_2. In order to recover fully independent elastic constants, higher order terms in the gradients of $Q_{\alpha\beta}$ must be included in either (21) or (35) for the free energy.

4.2. The LB method for liquid crystals

We now discuss the application of the LB method to the modelling of liquid crystals. A short review of the LB method for isotropic fluids is given in the appendix.

4.2.1. The problem. The LB method may be considered to arise from a discretization of the Boltzmann equations (e.g. He and Luo (1997)). However, although work has been undertaken to develop a kinetic theory of a gas of non-spherical particles (e.g. Curtiss (1956)), such a theory seems unlikely to form the basis of a kinetic theory of an ordered liquid phase. The relationship between the molecular properties and the macroscopic behaviour of LCs is complex. Thus, for example, the derivation of the macroscopic viscosities from the microscopic simulations described in earlier sections is not straightforward. There are two possible approaches; transport coefficients can be calculated from either equilibrium or non-equilibrium molecular dynamics. Rotational viscosities have been calculated from equilibrium molecular dynamics simulations (e.g. Allen *et al* (1996a), Cuetos *et al* (2002)), and work has been undertaken by Sollich *et al* (1989) using NEMD to calculate the Miesowicz viscosities. The equilibrium approach has the merit that, in principle, a single simulation can yield all the required coefficients; however, there remain unresolved technical problems regarding the correct method of extracting all the required information from the simulations. Theoretical work has been undertaken to derive the Leslie coefficients from molecular properties (e.g. Kuzuu and Doi (1983), Osipov and Terentjev (1989)) using statistical mechanical arguments.

Given the complexity of the relationship between the molecular behaviour and the macroscopic coefficients, the approach to developing a LB scheme for the nematic phases has adopted a top–down philosophy in which an LB scheme is designed to recover the required macroscopic equations rather than requiring the macroscopic equations to be emergent from some simplified mesoscopic dynamics. In order to adapt the LB method to represent a nematic LC, it is necessary to add additional degrees of freedom to the LB densities in order to carry information about orientational order; the LB densities must not only transport mass and momentum information between sites but also information about the orientational order of the fluid elements and the order parameter of the nematic. The schemes which are developed must then recover the equations associated with an appropriate macroscopic description of the nematic LC.

There have been essentially four approaches to this problem. Care *et al* (2000) recovered the ELP equations using a scheme in which the momentum density, f_i, is augmented by a

second Boltzmann equation for the propagation of a (two-dimensional) vector which carries the order information. Denniston *et al* (2001a) recover the Beris–Edwards equations by introducing a second Boltzmann equation which controls the evolution of a tensor order parameter; in the third approach Care *et al* (2003) also propagate a tensor density. Apart from the different target macroscopic equations, perhaps the principal difference between the latter two approaches lies in the way in which the coupling between the director and flow fields is achieved. In the approach of Denniston *et al* this coupling is achieved by (i) modifications to the equilibrium distribution function and (ii) forcing terms, principally to introduce the antisymmetric components to the stress tensor. Care *et al* (2003) achieve the coupling through (i) anisotropic scattering and (ii) forcing terms. In the most recent work by the latter group (Spencer and Care 2005) the forcing term is used to introduce all the coupling. The methods of Denniston *et al* (2004) and Spencer and Care (2005) appear to be of equivalent numerical complexity. One might argue that the equilibrium distribution function of a nematic is intrinsically isotropic for a real nematic, but within the LB method the inclusion of physical phenomena through forcing and through the equilibrium distribution function are essentially equivalent, the difference perhaps being a matter of taste. In this review we only describe the method of Denniston *et al* (2004) (section 4.2.3) and the method of Spencer and Care (2005) (section 4.2.4).

An important problem that needs to be considered when developing LB schemes is the widely differing time- and length-scales associated with the macroscopic parameters, i.e. the momentum, the order parameter and the director (e.g. Qian and Sheng (1998)). The order parameter changes on the shortest time-scale; this is typically of the order of 0.1 μs and over length-scales which may be as short as a few nanometres. The time-scale taken for the director to equilibrate depends upon the size of the system being considered, but for typical devices sizes of 10 μm it may take of the order of a second, whereas the time taken for the velocity to come to steady state may be of the order of 1 μs; this is consistent with a typical device Reynolds number of the order of 10^{-6}. Handling these large differences in time-scale is a particular challenge when, for example, modelling switching in a real device geometry. One approach is to run the LB at the shortest time-scale and completely resolve all the dynamics, but this is computationally very inefficient, and it therefore preferable to operate the LB solver for the momentum on a different time-scale to that for the director field. This is equivalent to the approach which is adopted with conventional solvers (e.g. Svensek and Zumer (2002)). Care must also be taken to correctly recover the dynamics of the order parameter, and this is an area of current research.

4.2.2. LB scheme for the ELP formalism. We mention briefly a scheme proposed by Care *et al* (2000) which used two coupled LB equations to recover the ELP equations. In Care *et al*'s (2000) scheme, one of the LB equations carried the momentum and the second carried a vector density corresponding to the director field. They presented results demonstrating the correct recovery of the Miesowicz viscosities (e.g. deGennes and Prost (1993)) and the flow alignment of the director in a shear flow. However, the approach was limited because the director was only two-dimensional and could not readily be generalized to three dimensions. Additionally, mapping onto the ELP equations limited the method to applications where changes in the order parameter were not significant. However, the work did introduce the anisotropic scattering matrix which was used in the method laid out in Care *et al* (2003).

4.2.3. LB scheme for Beris–Edwards formalism. Denniston and co-workers have developed (Denniston *et al* 2000, 2001a, 2004) a LB scheme for nematic LCs based on

Beris and Edwards (1994) scheme described in section 4.1.2 which recovers the equations for the flow of a nematic LC with variable order parameter.

Denniston *et al*'s (2001a) method is based on two coupled LB schemes, one for a scalar distribution $f_i(\mathbf{r})$ from which the density and momentum can be recovered in the usual way (see equations (A3)) and one for a tensor distribution $\mathbf{G}_i(\mathbf{r})$ from which the order tensor is recovered through

$$\mathbf{Q} = \sum_i \mathbf{G}_i. \tag{37}$$

One can think of the tensor density as carrying information about the ordering of that population of the fluid 'element' on the velocity link i, associated with a particular position and time. Hence the densities of a standard LB scheme have been generalized to carry information about the order associated with the fluid in addition to the density and momentum. These two distributions are evolved using

$$f_i(\mathbf{r} + \mathbf{c}_i\Delta t, t + \Delta t) - f_i(\mathbf{r}, t) = \frac{\Delta t}{2}[\mathcal{C}_{f_i}(\mathbf{r}, t, \{f_i\}) + \mathcal{C}_{f_i}(\mathbf{r} + \mathbf{c}_i\Delta t, t + \Delta t, \{f_i^*\})], \tag{38}$$

$$\mathbf{G}_i(\mathbf{r} + \mathbf{c}_i\Delta t, t + \Delta t) - \mathbf{G}_i(\mathbf{r}, t) = \frac{\Delta t}{2}[\mathcal{C}_{\mathbf{G}_i}(\mathbf{r}, t, \{\mathbf{G}_i\}) + \mathcal{C}_{\mathbf{G}_i}(\mathbf{r} + \mathbf{c}_i\Delta t, t + \Delta t, \{\mathbf{G}_i^*\})]. \tag{39}$$

This is an implicit LB scheme where $\{f_i^*\}$ and $\{\mathbf{G}_i^*\}$ are first order approximations to $f_i(\mathbf{r} + \mathbf{c}_i\Delta t, t + \Delta t)$ and $\mathbf{G}_i(\mathbf{r} + \mathbf{c}_i\Delta t, t + \Delta t)$, respectively. The latter quantities are obtained from equations (38) and (39) with $\{f_i^*\}$ and $\{\mathbf{G}_i^*\}$ set to $\{f_i\}$ and $\{\mathbf{G}_i\}$. The implicit scheme is used in order to suppress a first order term of order $O(\Delta t)$ which contributes a term to the viscosity in the standard LB schemes (known as the lattice viscosity). The authors also report that this approach improves stability.

The collision operators are taken to be of the form

$$\begin{aligned} \mathcal{C}_{f_i} &= -\frac{1}{\tau_f}[f_i(\mathbf{r}, t) - f_i^{(0)}(\mathbf{r}, t, \{f_i\})] + p_i(\mathbf{r}, t, \{f_i\}), \\ \mathcal{C}_{\mathbf{G}_i} &= -\frac{1}{\tau_g}[\mathbf{G}_i(\mathbf{r}, t) - \mathbf{G}_i^{(0)}(\mathbf{r}, t, \{\mathbf{G}_i\})] + \mathbf{M}_i(\mathbf{r}, t, \{\mathbf{G}_i\}), \end{aligned} \tag{40}$$

which both include a BGK type relaxation and a forcing term. In order to complete the definition of the scheme it is necessary to define the equilibrium distribution functions and the forcing terms. The required macroscopic equations may be recovered by making the following constraints on the equilibrium distribution for the momentum density

$$\sum_i f_i^{(0)} = \rho \qquad \sum_i f_i^{(0)} c_{i\alpha} = \rho u_\alpha \qquad \sum_i f_i^{(0)} c_{i\alpha} c_{i\beta} = -\sigma_{\alpha\beta} + \rho u_\alpha u_\beta. \tag{41}$$

The second moment is used to introduce the symmetric component of the stress tensor, $\sigma_{\alpha\beta}$. It should be noted that the second moment of the distribution function in an LB schemes is intrinsically symmetric and hence the antisymmetric part of the stress tensor can only be introduced through a forcing term. This is achieved by defining

$$\sum_i p_i = 0 \qquad \sum_i p_i c_{i\alpha} = \partial_\beta \sigma^a_{\alpha\beta} \qquad \sum_i p_i c_{i\alpha} c_{i\beta} = 0, \tag{42}$$

where $\sigma^a_{\alpha\beta}$ is the antisymmetric part of the stress tensor defined in equation (24) and p_i is the forcing term introduced in the first of equations (40). The equilibrium distribution function for the order parameter is chosen to have moments

$$\sum_i \mathbf{G}_i^{(0)} = \mathbf{Q} \qquad \sum_i \mathbf{G}_i^{(0)} c_{i\alpha} = \mathbf{Q} u_\alpha \qquad \sum_i \mathbf{G}_i^{(0)} c_{i\alpha} c_{i\beta} = \mathbf{Q} u_\alpha u_\beta. \tag{43}$$

In order to recover the target macroscopic equations, the forcing for the order parameter evolution is required to satisfy

$$\sum_i \mathbf{M}_i = \Gamma \mathbf{H}(\mathbf{Q}) + \mathbf{S}(\mathbf{W}, \mathbf{Q}) \qquad \sum_i \mathbf{M}_i c_{i\alpha} = \left(\sum_i \mathbf{M}_i \right) u_\alpha. \tag{44}$$

The conditions on the equilibrium and forcing functions can be satisfied by assuming the following general forms

$$\begin{aligned} f_i^{(0)} &= A_s + B_s u_\alpha c_{i\alpha} + C_s u_\alpha u_\alpha + D_s u_\alpha u_\beta c_{i\alpha} c_{i\beta} + E_{s\alpha\beta} c_{i\alpha} c_{i\beta}, \\ \mathbf{G}_i^{(0)} &= \mathbf{J}_s + \mathbf{K}_s u_\alpha c_{i\alpha} + \mathbf{L}_s u_\alpha u_\alpha + \mathbf{N}_s u_\alpha u_\beta c_{i\alpha} c_{i\beta}, \\ p_i &= T_s \partial_\beta \tau_{\alpha\beta} c_{i\alpha}, \\ \mathbf{M}_i &= \mathbf{R}_s + \mathbf{S}_s u_\alpha c_{i\alpha}. \end{aligned} \tag{45}$$

Precise expressions for the coefficients in these expressions can be found in Denniston *et al* (2001a).

4.2.4. LB scheme for Qian–Sheng formalism. We now describe an the LB scheme of Spencer and Care (2005) which takes the Qian–Sheng equations as the target equations, rather than those of Beris–Edwards. The scheme is able to recover the full tensorial coupling of the order tensor to the velocity gradient tensor. One merit of the Qian–Sheng approach is that the equations map more directly onto the ELP equations for which the coefficients are known for a number of real LCs.

In order to recover the Qian–Sheng equations of section 4.1.3 two LBGK algorithms are used, one for the evolution of the momentum based on a scalar density $f_i(\mathbf{x}, t)$ and a second LBGK scheme based on a tensor density $g_{i\alpha\beta}(\mathbf{x}, t)$ to recover the order tensor evolution. The principal reason for separating the momentum and order evolution algorithms is the very large difference in time-scales between the two processes, as was discussed in section 4.2.1. In each algorithm, forcing terms are used to recover the required form of the stress tensor and order evolution equations. This approach is more straightforward to implement than the anisotropic scattering method used in an earlier work (Care *et al* 2003).

The LBGK algorithm for an isotropic fluid may be written in the form

$$f_i\left(\mathbf{x} + \mathbf{c}_i \delta, t + \delta\right) = f_i\left(\mathbf{x}, t\right) - \frac{1}{\tau_p}\left(f_i\left(\mathbf{x}, t\right) - f_i^{(eq)}\left(\mathbf{x}, t\right)\right) + \phi_i, \tag{46}$$

where $f_i(\mathbf{x}, t)$ is the distribution function for particles with velocity $\mathbf{c}_i$ at position $\mathbf{x}$ and time t, and δ is the time increment. $f_i^{(eq)}(\mathbf{x}, t)$ is the equilibrium distribution function and τ_p is the LBGK relaxation parameter for the momentum. The fluid density and velocity are determined by the moments of the distribution function,

$$\sum_i f_i \begin{bmatrix} 1 \\ c_{i\alpha} \end{bmatrix} = \begin{bmatrix} \rho(\mathbf{x}, t) \\ \rho u_\alpha(\mathbf{x}, t) \end{bmatrix}. \tag{47}$$

The mesoscale equilibrium distribution function appropriate for recovering the correct hydrodynamics of incompressible fluids ($M \ll 1$) is

$$f_i^{(eq)} = t_i \rho \left[1 + \frac{c_{i\alpha} u_\alpha}{c_s^2} + u_\alpha u_\beta \left(\frac{c_{i\alpha} c_{i\beta} - c_s^2 \delta_{\alpha\beta}}{2 c_s^4} \right) \right], \tag{48}$$

where t_i are lattice weights. t_i, $\mathbf{c}_i$, c_s are all dependent upon the choice of lattice; appropriate values of these parameters are summarized in Dupin *et al* (2004). An analysis of the standard isotropic algorithm identifies the lattice pressure and kinematic viscosity to be given by

$$P = \rho c_s^2 \qquad \nu = \frac{c_s^2}{2}\left(2\tau_p - 1\right)\Delta t. \tag{49}$$

ϕ_i is a forcing term which is chosen to recover the required terms in the stress tensor (equation (30)) for a nematic liquid crystal and is defined to be

$$\phi_i = t_i c_{i\lambda} \partial_\beta F_{\lambda\beta}, \tag{50}$$

where

$$F_{\alpha\beta} = \frac{\Delta t}{c_s^2}\Bigg[\sigma^d_{\alpha\beta} + \sigma^{EM}_{\alpha\beta} + \beta_1 Q_{\alpha\beta} Q_{\mu\nu} A_{\mu\nu} + \beta_5 Q_{\alpha\mu} A_{\mu\beta} + \beta_6 Q_{\beta\mu} A_{\mu\alpha} + \frac{\mu_2 h_{\alpha\beta}}{2\mu_1} - \frac{\mu_2 \varepsilon_{\alpha\beta\gamma}\lambda_\gamma}{2\mu_1} - Q_{\alpha\mu} h_{\mu\beta} + Q_{\alpha\mu}\varepsilon_{\mu\beta\gamma}\lambda_\gamma + \frac{\mu_2 Q_{\alpha\mu} A_{\mu\beta}}{2} + Q_{\beta\mu} h_{\mu\alpha} - Q_{\beta\mu}\varepsilon_{\mu\alpha\gamma}\lambda_\gamma - \frac{\mu_2 Q_{\beta\mu} A_{\mu\alpha}}{2}\Bigg] \tag{51}$$

with analysis identifying (see Spencer and Care (2005))

$$P = \rho c_s^2 + \frac{\mu_2 \lambda}{2\mu_1} \qquad \rho c_s^2 (2\tau_p - 1) = \beta_4 - \frac{\mu_2^2}{4\mu_1}. \tag{52}$$

In order to recover the order evolution equation (29), we retain the simple LBGK form but replace the scalar density $f_i(\mathbf{x}, t)$ with a tensor distribution $g_{i\alpha\beta}(\mathbf{x}, t)$ evolving according to

$$g_{i\alpha\beta}(\mathbf{x} + \mathbf{c}_i\delta, t + \delta) = g_{i\alpha\beta}(\mathbf{x}, t) - \frac{1}{\tau_Q}(g_{i\alpha\beta}(\mathbf{x}, t) - g^{(eq)}_{i\alpha\beta}(\mathbf{x}, t)) + \chi_{i\alpha\beta}. \tag{53}$$

Here $g^{(eq)}_{i\alpha\beta}(\mathbf{x}, t)$ is the equilibrium order distribution function and τ_Q the LBGK relaxation parameter for the order. The lowest moment of the order distribution function and its associated equilibrium function are defined so as to recover the order tensor of unit trace, $S_{\alpha\beta}$.

$$S_{\alpha\beta} = \sum_i g_{i\alpha\beta} = \sum_i g^{(eq)}_{i\alpha\beta}, \tag{54}$$

which is simply related to the dimensionless zero trace order parameter, $\mathbf{Q}$, through the relation

$$Q_{\alpha\beta} = \frac{3S_{\alpha\beta} - \delta_{\alpha\beta}}{2}. \tag{55}$$

The equilibrium order distribution is taken to be

$$g^{(eq)}_{i\alpha\beta} = t_i S_{\alpha\beta}\left[1 + \frac{c_{i\alpha}u_\alpha}{c_s^2} + u_\alpha u_\beta\left(\frac{c_{i\alpha}c_{i\beta} - c_s^2\delta_{\alpha\beta}}{2c_s^4}\right)\right]. \tag{56}$$

$t_i, c_{i\alpha}, c_s^2$ are the same lattice parameters defined for the momentum evolution. The forcing term, $\chi_{i\alpha\beta}$, is chosen to provide the rotational forces required to correctly recover equation (29):

$$\chi_{i\alpha\beta} = \frac{2t_i}{3}\left[\frac{h_{\alpha\beta}}{\mu_1} - \frac{L_1\partial_\lambda\partial_\lambda Q_{\alpha\beta}}{\mu_1} - \frac{\lambda\delta_{\alpha\beta}}{\mu_1} - \frac{\varepsilon_{\alpha\beta\gamma}\lambda_\gamma}{\mu_1} - \frac{\mu_2 A_{\alpha\beta}}{2\mu_1} + \varepsilon_{\alpha\epsilon\lambda}\omega_\epsilon Q_{\lambda\beta} + \varepsilon_{\beta\epsilon\lambda}\omega_\epsilon Q_{\alpha\lambda}\right]. \tag{57}$$

The analysis of Spencer and Care (2005) identifies the key relation,

$$\Delta t\frac{c_s^2}{2}(2\tau_Q - 1) = \frac{L_1}{\mu_1}. \tag{58}$$

The scheme involves two coupled LB algorithms which may be run independently; for example, if the effect of flow is to be ignored or only static equilibrium configurations are desired, running the $g_{i\alpha\beta}$ scheme alone will suffice. In practice, for typical device geometries, the flow fields evolve on a much faster time-scale than does the director field; to model such systems the momentum is evolved to steady state between each time step of the order evolution equation. Although the time taken for the momentum to reach equilibrium is significantly shorter than the times step of the order evolution equation, the loss of accuracy in this approach is small. A detailed Chapman–Enskog analysis of the algorithm is presented in Spencer and Care (2005).

4.2.5. Applications of the LB method. The LB schemes described above have been used to model a range of problems in nemato-dynamics.

Denniston *et al* (2001b) studied the kinetics of the nematic–isotropic transition in a two-dimensional LC. They demonstrated that the time dependence of the correlation function, energy density and number of defects obeys dynamic scaling laws with a growth exponent of 1/2 as is predicted by dimensional analysis. It was noted that the exponent is not recovered if the length-scale of the defects becomes too small; in this case the defects become pinned to the lattice. This highlights the importance of correctly describing phenomena on different length-scales; this may be a source of severe computational difficulties in many LC systems. Denniston *et al* (2001c) studied LCs in a Poiseuille flow and reported two steady states at low Reynolds number; the state which was observed depended upon the flow history and the shear rate. At high shear-rates, shear thinning and log-rolling were observed.

Denniston and Yeomans (2001) used the LB scheme described in section 4.2.3 to study a simplified model of a bistable nematic device. In particular, they investigated the effect of surface flexoelectric switching. Toth *et al* (2002a) studied the effects of back-flow on the motion of defects in a LC and subsequently Denniston *et al* (2002) and Toth *et al* (2002b) studied the influence of flow and back-flow on the switching of common device structures. Marenduzzo *et al* (2003) studied the influence of flow in a hybrid cell and observed shear banding close to the nematic–isotropic transition temperature. Jung *et al* (2003) and Toth *et al* (2003) studied domain growth in nematic LCs. The LB scheme of Care *et al* (2003) has been adapted to model a mixture of an isotropic fluid and a nematic liquid crystal by introducing additional terms to describe the interface between the two fluids (Care *et al* 2003, Lishchuk *et al* 2004). The method is based on the description of the nematic–isotropic interface developed by Rey (2001). The LB scheme described in section 4.2.4 has been used by Spencer and Care (2005) to study the motion of defects in a zenithal bistable device (Wood *et al* 2000) during switching by an external electric field. This latter example illustrates the ability of the LB method to model systems with complex boundary conditions and suggests that the detailed modelling of full devices at meso- to continuum length-scales is close to being realized.

5. Conclusions and future directions

This review has highlighted the significant progress made in the computer simulation of LCs at each of the micro-, meso- and continuum length-scales. From this it is apparent that modelling in *each* of these regimes still has important contributions to make in furthering the understanding and applications of LCs.

The microscopic regime continues to provide insight into behaviour which is often difficult to observe experimentally. Additionally, it provides a means of exploring exciting developments such as novel LC phases (e.g. biaxial, ferroelectric), the role of formulation and the behaviour of LCs in regions of complex ordering (e.g. defects, microconfinement). Importantly, use of all-atom models to determine mesoscopic parameters such as Frank elastic and flexoelectric coefficients is now becoming achievable.

Meso- and macroscopic LC simulations have now reached the state of maturity at which they can be used to undertake predictive modelling of full device behaviour. Unfortunately, their applicability is still limited by incomplete experimental data on the many material parameters needed fully to characterize a LC or LC mixture. Additionally, the use of such models should be tempered by the understanding that numerical stability does not always imply the validity of the underlying mathematical model. This is particularly evident in regions

of high gradients in macroscopic parameters, where bulk continuum descriptions become inappropriate and recourse to a molecular basis is needed.

The outstanding problem in this field remains the development of schemes which cross all the contributing length- and time-scales. Thus the ability to design a molecule and predict both its macroscopic properties and its consequent behaviour within a device is still a long way from being achieved. This arises, in part, due to the non-linear coupling between the different scales of mesogenic phenomena, as discussed in section 1. One of the central issues is that molecular fluids such as LCs are intrinsically many-body systems. Hence, each constituent molecule has degrees of freedom which it is difficult to integrate out in a way that yields a well-behaved, general-purpose coarse grained model. To some extent, this key modelling difficulty is simply a reflection of the properties of LCs which make them technologically important; the macroscopic response of an LC to external fields has a complex, non-linear, dependence on a spectrum of behaviours.

The development of hybrid schemes which allow information exchange between LC models covering different length- and time-scales is now a pressing need. Preliminary work on such schemes has already been undertaken for simple fluids (e.g. Delgado-Buscalioni and Coveney (2004)), and extension of these approaches to more complex materials appears achievable. Such a development, when combined with predictive modelling of material parameters, will open up the possibility of true 'atom-to-device' modelling. Furthermore, there is increasing demand for such modelling capabilities; the next generation of LC-based devices will employ surface features of tens of nanometres embedded in cells which are several micrometres in extent. Hybrid methodologies, able to operate simultaneously across the current regimes, will be crucial for the potential of modelling to be realized in the design and optimization of such devices.

Acknowledgments

This review has been greatly influenced by our interactions over many years with many researchers in this wide field. Particularly helpful have been discussions and collaborations with Mike Allen, Mike Cates, John Goodby, Jim Henderson, Ian Halliday, George Jackson, Cliff Jones, Geoffrey Luckhurst, Damien McDonnell, Andrew Masters, Richard Miller, Nigel Mottram, Maureen Neal, Yuzuru Sato, Tim Sluckin, Paulo Teixeira, Masamitsu Uehara, Mark Wilson, Julia Yeomans and Claudio Zannoni. We would also like to acknowledge the contributions made by the students and postdoctoral researchers we have worked with in our group. In particular, however, we wish to thank Fred Barmes and Tim Spencer for the important contributions they have made towards the preparation of this document.

Appendix. The LB method for isotropic fluids

The LB method has been developed and extensively studied as a mesoscopic method of simulating isotropic fluids (e.g. Qian *et al* (1992), Hou *et al* (1995), Boghosian (1998), Succi (2001)). The equations of the LB algorithm may be derived in a variety of different ways; one of the most physically illuminating is that of He and Luo (1997), who demonstrate that the equations may be derived by an appropriate discretization of an underlying Boltzmann equation. The particular strengths of the method lie in the modelling of flow in complex geometries (e.g. Koponen *et al* (1998)) or in multi-component flows (e.g. Swift *et al* (1996), Dupin *et al* (2003)). It is in this class of application that LB solvers for LC materials may have particular advantages. We begin by summarizing the LBGK (e.g. Qian *et al* (1992))

algorithm which is a robust, and commonly used, LB algorithm for simulating isotropic fluids. The algorithm is a LB implementation of the Bhatnagar *et al* (1954) approximation which was developed in the classical kinetic theory of gases (e.g. Chapman and Cowling (1995)).

In the LB method, the continuum fluid is represented by a set of densities, $f_i(\mathbf{r}, t)$, which populate a regular lattice defined by a basis of velocity vectors, $c_{i,\alpha}$; there are a variety of choices for the velocity vectors. Some care must be taken to minimize artefacts of the lattice being evident in the macroscopic results, and this is usually achieved by including appropriate weights in the definition of the equilibrium distribution function as discussed below. In two dimensions, a square lattice with nearest and next nearest neighbours is commonly used. A density is placed on a rest link giving nine velocities in total; hence the system is referred to as D2Q9, implying a system in two dimensions with a co-ordination number of 9. The core algorithm is written

$$f_i(\mathbf{r} + \delta\mathbf{c}_i, t + \delta) = f_i(\mathbf{r}, t) + \frac{f_i(\mathbf{r}, t) - f_i^{(0)}(\mathbf{r}, t; \rho, \mathbf{u})}{\tau} + \phi_i, \tag{A1}$$

which represents three of the steps in an LB algorithm: collision, forcing and propagation. Thus the density, $f_i(\mathbf{r}, t)$, at lattice site $\mathbf{r}$ and time t is

(i) perturbed by the addition of a collision term (the second term on the right-hand side of equation (A1)),
(ii) perturbed by the addition of a forcing term (ϕ_i),
(iii) propagated to form the density $f_i(\mathbf{r} + \delta\mathbf{c}_i, t + \delta)$ at lattice site $(\mathbf{r} + \delta\mathbf{c}_i)$ at time $(t + \delta)$,

where δ is the increment in time. The quantity $f_i^{(0)}(\mathbf{r}, t; \rho, \mathbf{u})$ is an equilibrium distribution function which may be thought of as a discrete form of a Maxwell–Boltzmann distribution for a fluid of density ρ moving uniformly at velocity $\mathbf{u}$. The equilibrium distribution function may be written in the form (Qian *et al* 1992)

$$f_i^{(0)} = \rho t_i \left[1 + \frac{1}{c_s^2} u_\alpha c_{i\alpha} + \frac{1}{2c_s^2} u_\alpha u_\beta \left(\frac{c_{i\alpha} c_{i\beta}}{c_s^2} - \delta_{\alpha\beta}\right)\right], \tag{A2}$$

where, in D2Q9, $t_0 = 4/9$, $t_1 = 1/9$ and $t_2 = 1/36$ and the velocity of sound $c_s = 1/\sqrt{3}$. $f_i^{(0)}$ is a function of the macroscopic variables ρ and $\mathbf{u}$ which are recovered after the propagation step (and before the collision step) by taking the moments

$$\begin{aligned} \rho(\mathbf{r}, t) &= \sum_i f_i(\mathbf{r}, t), \\ \rho u_\alpha(\mathbf{r}, t) &= \sum_i c_{i\alpha} f_i(\mathbf{r}, t). \end{aligned} \tag{A3}$$

For the D2Q9 lattice the summation is over the $Q = 9$ velocity directions at each site. It is this projection step which yields the macroscopic quantities from the mesoscopic densities, f_i. The equilibrium distribution function is normally chosen to have the following moments

$$\begin{aligned} \sum_i f_i^{(0)}(\mathbf{r}, t) &= \rho(\mathbf{r}, t), \\ \sum_i c_{i\alpha} f_i^{(0)}(\mathbf{r}, t) &= \rho u_\alpha(\mathbf{r}, t), \\ \sum_i c_{i\alpha} c_{i\beta} f_i^{(0)}(\mathbf{r}, t) &= \delta_{\alpha\beta} \rho c_s^2 + \rho u_\alpha u_\beta. \end{aligned} \tag{A4}$$

The weights, t_p, in the equilibrium distribution function (A2) are determined by the requirement to recover these moments and also to achieve isotropy up to fourth order in the velocity

tensors; the latter requirement minimizes the effect of the underlying lattice in the macroscopic quantities. If ρc_s^2 is identified as the isotropic pressure in the system, the right-hand side of the last equation in (A4) represents the equilibrium momentum flux density tensor. Given this identification of the pressure, it can be seen that the fluid modelled by this standard LB algorithm is weakly compressible. It can be shown, either by a Chapman–Enskog-type analysis (e.g. Hou *et al* (1995), Chapman and Cowling (1995)) or by a more direct Taylor series analysis (e.g. Swift *et al* (1996)) that the algorithm recovers the continuity equation and Navier–Stokes equation for the momentum evolution of an incompressible fluid to second order in $\mathbf{u}$ in the bulk of the fluid.

The closure of the simulation at the boundaries can be achieved in a variety of ways. The simplest approach is to impose periodic boundary conditions, as for molecular simulations. However, most simulations of physical interest require the explicit presence of a boundary and also a mechanism for enforcing flow. It is important to note that an LB scheme does not impose boundary conditions in the same way as a conventional numerical solver. Thus, during the propagation step in an LB solver there is the problem of constructing densities on the links which flow into the simulation region. There are a variety of methods for imposing the effects of a boundary on the fluid; the simplest is a bounce back condition in which the densities which propagate onto the boundary sites undergo specular reflection. To lowest order in the velocity this recovers a no-slip boundary condition. More sophisticated closure schemes include mid-link bounce back (e.g. He *et al* (1997)) and schemes which ensure that the stress tensor is correctly recovered on the boundary (Hammond *et al* 2002). Flow in the simulation is achieved either by modification to the densities on the boundaries or by imposing a suitable forcing term, ϕ_i, in equation (A1). Thus one complete iteration of the LB algorithm consists of the following steps: collision, boundary closure, forcing, propagation and projection. The scheme just described recovers the Navier–Stokes equations for an incompressible isotropic fluid and provides an algorithm which is straightforward to implement for such systems.

LB methods have been extensively studied to model the phase separation and coexistence of binary (e.g. Swift *et al* (1996), Shan and Chen (1993), Gunstensen *et al* (1991)) and multi-component fluids (e.g. Dupin *et al* (2003)). In these methods each lattice site may be populated by densities of more than one type. In the Gunstensen approach the different densities are identified directly with each type of fluid and a standard equilibrium distribution function is retained. Additional local rules are imposed at mixed sites which (i) achieve colour separation and (ii) apply a perturbation to create a surface of tension between the two fluids. This method is able to model fluids which are fully separated and also droplet coalescence or break up. However it is unable to recover the dynamics of phase separation.

This latter problem can be addressed by the approach of (Swift *et al* 1996), in which they employ (i) a density f_i which recovers the density and momentum of the total fluid and (ii) a density g_i which obeys a LB equation designed to recover a convection diffusion equation for the density difference. The equilibrium distribution function in this method is constructed to recover a modified form of equation (A4):

$$\sum_i c_{i\alpha} c_{i\beta} f_i^{(0)}(\mathbf{r}, t) = P_{\alpha\beta} + \rho u_\alpha u_\beta, \tag{A5}$$

where $P_{\alpha\beta}$ is a pressure tensor derived directly from a free energy expression which includes a Cahn and Hilliard (1958) description of the non-equilibrium phase separation dynamics. The approach of Swift *et al* (1996) explicitly identifies a chemical potential difference which drives the phase separation. The Gunstensen *et al* (1991) approach can potentially achieve sharper interfaces than those achieved by Swift *et al* (1996) which may be considered more

appropriate at mesoscopic length-scales but pays the penalty of not having an explicit form for the chemical potential difference.

A commonly used alternative approach to generating an interface has been presented by Shan and Chen (1993) in which there are interactions between densities at different sites. This method recovers spontaneous phase separation although momentum is now conserved globally rather than locally.

Another application where LB methods may have advantages over conventional computational fluid dynamics (CFD) is that of modelling the interaction of fluids with embedded particles (e.g. colloidal suspensions). Once again there are a variety of approaches, and we refer the reader to Ladd and Verberg's (2001) recent review. These approaches are of interest in the context of the current paper since the development of LB methods allows the interaction of a nematic LC with a colloidal particle or an isotropic fluid (e.g. Lishchuk and Care (2004)) to be simulated.

References

Acharya B R, Primak A and Kumar S 2004 *Phys. Rev. Lett.* **92** 145506
Adams D J, Luckhurst G R and Phippen R W 1987 *Mol. Phys.* **61** 1575
Allen M P 1990 *Liq. Cryst.* **8** 499
Allen M P 1993 *Phil. Trans. R. Soc. Lond.* A **344** 323
Allen M P, Camp P J, Mason C P, Evans G T and Masters A J 1996a *J. Chem. Phys.* **105** 11175
Allen M P, Evans G T, Frenkel D and Mulder B M 1993 *Adv. Chem. Phys.* **86** 1
Allen M P and Mason C P 1995 *Mol. Phys.* **86** 467
Allen M P and Tildesley D J 1986 *Computer Simulation of Liquids* (Oxford: Oxford University Press)
Allen M P, Warren M A, Wilson M R, Sauron A and Smith W 1996b *J. Chem. Phys.* **105** 2850
Allen M P and Wilson M R 1989 *J. Comput. Aided Mol. Des.* **3** 335
Andrienko D, Germano G and Allen M P 2001 *Phys. Rev.* E **63** 041701
Antypov D and Cleaver D J 2003 *Chem. Phys. Lett.* **377** 311
Antypov D and Cleaver D J 2004a *J. Phys.: Condens. Matter* **16** S1887
Antypov D and Cleaver D J 2004b *J. Chem. Phys.* **120** 10307
Ayton G and Patey G N 1995 *J. Chem. Phys.* **102** 9040
Ayton G and Patey G N 1996 *Phys. Rev. Lett.* **76** 239
Ayton G, Wei D Q and Patey G N 1997 *Phys. Rev.* E **55** 447
Banerjee S, Griffiths R B and Widom M 1998 *J. Stat. Phys.* **93** 109
Barmes F and Cleaver D J 2005 *Phys. Rev.* E **71** 021705
Barmes F, Ricci M, Zannoni C and Cleaver D J 2003 *Phys. Rev.* E **68** 021708
Bates M A 1998 *Phys. Rev.* E **64** 051702
Bates M A and Frenkel D 1998a *Phys. Rev.* E **57** 4824
Bates M A and Frenkel D 1998b *J. Chem. Phys.* **109** 6193
Bates M A and Luckhurst G R 1998 *J. Chem. Phys.* **104** 6696
Bates M A and Luckhurst G R 1999 *J. Chem. Phys.* **110** 7087
Bemrose R A, Care C M, Cleaver D J and Neal M P 1997 *Mol. Phys.* **90** 625
Berardi R, Emerson A P J and Zannoni C 1993 *J. Chem. Soc. Faraday Trans.* **89** 4069
Berardi R, Fava C and Zannoni C 1998 *Chem. Phys. Lett.* **297** 8
Berardi R, Fehevari M and Zannoni C 1999 *Mol. Phys.* **97** 1173
Berardi R, Muccioli L and Zannoni C 2004 *Chem. Phys. Chem.* **5** 104
Berardi R, Orlandi S, Photinos D J, Vanarakas A G and Zannoni C 1996a *PCCP* **4** 770
Berardi R, Orlandi S and Zannoni C 1996b *Chem. Phys. Lett.* **261** 357
Berardi R, Orlandi S and Zannoni C 2003 *Phys. Rev.* E **67** 041708
Berardi R, Ricci M and Zannoni C 2001 *Chem. Phys. Chem.* **2** 443
Berardi R, Ricci M and Zannoni C 2004 *Ferroelectrics* **309** 3
Berardi R and Zannoni C 2000 *J. Chem. Phys.* **113** 5971
Berggren E, Zannoni C, Chiccoli C, Pasini P and Semeria F 2003 *Phys. Rev.* E **50** 2929
Beris A N and Edwards B J 1994 *Thermodynamics of Flowing Systems* (Oxford: Oxford University Press)
Berne B J and Pechukas P 1972 *J. Chem. Phys.* **56** 4213

Bhatnagar P L, Gross E P and Krook M 1954 *Phys. Rev.* **94** 511
Bhethanabotla V R and Steele W 1987 *Mol. Phys.* **60** 249
Billeter J L and Pelcovits R A 2000 *Liq. Cryst.* **27** 1151
Biscarini F, Chiccoli C, Pasini P, Semeria F and Zannoni C 1995 *Phys. Rev. Lett.* **75** 1803
Biscarini F, Zannoni C, Chiccoli C and Pasini P 1991 *Mol. Phys.* **73** 439
Boghosian B M (ed) 1998 *Int. J. Mod. Phys.* (*Proc. 7th Int. Conf. on the Discrete Simulation of Liquids*) vol 9 (Singapore: World Scientific)
Bolhuis P and Frenkel D 1997 *J. Chem. Phys.* **106** 666
Born M 1916 *Sits. Phys. Maths.* **25** 614
Brown J T, Allen M P, Martín del Río E and de Miguel E 1998 *Phys. Rev.* E **57** 6685
Cacelli I, Campanile S, Prampolini G and Tani A 2002 *J. Chem. Phys.* **117** 448
Cahn J W and Hilliard J E 1958 *J. Chem. Phys.* **28** 258
Camp P J and Allen M P 1996 *Physica* A **229** 410
Camp P J and Allen M P 1997 *J. Chem. Phys.* **106** 6681
Camp P J, Allen M P, Bolhuis P G and Frenkel D 1997 *J. Chem. Phys.* **106** 9270
Camp P J, Allen M P and Masters A J 1996a *J. Chem. Phys.* **11** 9871
Camp P J, Mason C P and Allen M P 1996b *J. Chem. Phys.* **105** 2837
Care C M, Halliday I and Good K 2000 *J. Phys.: Condens. Matter* **12** L665
Care C M, Halliday I, Good K and Lishchuk S V 2003 *Phys. Rev.* E **67** 061703
Chalam M J, Gubbins K E, de Miguel E and Rull L F 1991 *Mol. Sim.* **7** 357
Chandrasekhar S 1992 *Liquid Crystals* (Cambridge: Cambridge University Press)
Chapman S and Cowling T G 1995 *The Mathematical Theory of Non-Uniform Gases* (Cambridge: Cambridge University Press)
Cheung D L, Clark S J and Wilson M R 2002 *Chem. Phys. Lett.* **356** 140
Cheung D L, Clark S J and Wilson M R 2004 *J. Chem. Phys.* **121** 9131
Chiccoli C, Pasini P, Semeria F and Zannoni C 1999 *Int. J. Mod. Phys.* C **10** 469
Chiccoli C, Pasini P and Zannoni C 1997 *Int. J. Mod. Phys.* B **11** 1937
Clark S J, Adam C J, Cleaver D J and Crain J 1997 *Liq. Cryst.* **22** 477
Cleaver D J and Allen M P 1991 *Phys. Rev.* A **43** 1918
Cleaver D J, Care C M, Allen M P and Neal M P 1996 *Phys. Rev.* E **54** 559
Cleaver D J and Tildesley D J 1994 *Mol. Phys.* **81** 781
Cook M J and Wilson M R 2000 *Liq. Cryst.* **27** 1573
Crain J and Komolkin A V 1999 *Adv. Chem. Phys.* **109** 39
Cross C W and Fung B M 1994 *J. Chem. Phys.* **101** 6839
Cuetos A, Ilnytskyi J M and Wilson M R 2002 *Mol. Phys.* **100** 3839
Curtiss C F 1956 *J. Chem. Phys* **24** 225
De Luca M D, Neal M P and Care C M 1994 *Liq. Cryst.* **16** 257
de Miguel E 1993 *Phys. Rev.* E **47** 3334
de Miguel E and Martín del Río E 2001 *J. Chem. Phys.* **115** 9072
de Miguel E and Martín del Río E 2003 *J. Chem. Phys.* **118** 1852
de Miguel E, Martín del Río E, Brown J T and Allen M P 1996 *J. Chem. Phys.* **105** 4234
de Miguel E, Rull L F, Chalam M J and Gubbins K E 1991a *Mol. Phys.* **74** 405
de Miguel E, Rull L F, Chalam M J and Gubbins K E 1991b *Mol. Phys.* **72** 593
de Miguel E, Rull L F, Chalam M K and Gubbins K E 1990 *Mol. Phys.* **71** 1223
de Gennes P G and Prost J 1993 *The Physics of Liquid Crystals* (Oxford: Clarendon)
Delgado-Buscalioni R and Coveney P V 2004 *Phil. Trans. R. Soc. Lond. Ser. A: Math. Phys. Eng. Sci.* **362** 1639
Denniston C, Marenduzzo D, Orlandini E and Yeomans J M 2004 *Phil. Trans. R. Soc. Lond. Ser. A: Math. Phys. Eng. Sci.* **362** 1745
Denniston C, Orlandini E and Yeomans J M 2000 *Eur. Phys. Lett.* **52** 481
Denniston C, Orlandini E and Yeomans J M 2001a *Phys. Rev.* E **63** 056702
Denniston C, Orlandini E and Yeomans J M 2001b *Phys. Rev.* E **64** 021701
Denniston C, Orlandini E and Yeomans J M 2001c *Comp. Theor. Polym. Sci.* **11** 389
Denniston C, Toth G and Yeomans J M 2002 *J. Stat. Phys.* **107** 187
Denniston C and Yeomans J M 2001 *Phys. Rev. Lett.* **87** 275505
Dewar A and Camp P J 2004 *Phys. Rev.* E **70** 011704
Dogic Z and Fraden S 1997 *Phys. Rev. Lett.* **78** 2417
Dogic Z, Frenkel D and Fraden S 2000 *Phys. Rev.* E **62** 3925
Doi M 1981 *J. Polym. Sci.: Polym. Phys.* **19** 229

Domínguez H, Velasco E and Alejandre J 2002 *Mol. Phys.* **100** 2739
Dunmur D A, Fukuda A and Luckhurst G R 2001 *Physical Properties of Liquid Crystals: Nematics* (INSPEC)
Dupin M M, Halliday I and Care C M 2003 *J. Phys. A: Math. Gen.* **36** 8517
Dupin M M, Spencer T J, Halliday I and Care C M 2004 *Phil. Trans. R. Soc. Lond. Ser. A: Math. Phys. Eng. Sci.* **362** 1885
Earl D J, Ilnytskyi J and Wilson M R 2001 *Mol. Phys.* **99** 1719
Emerson A P J, Luckhurst G R and Whatling S G 1994 *Mol. Phys.* **82** 113
Eppenga R and Frenkel D 1984 *Mol. Phys.* **52** 1303
Espanol P and Revenga M 2003 *Phys. Rev.* E **67** 026705
Fabbri U and Zannoni C 1986 *Mol. Phys.* **58** 763
Frenkel D 1987 *Mol. Phys.* **60** 1
Frenkel D and Mulder B M 1985 *Mol. Phys.* **55** 1171
Frenkel D, Mulder B M and McTague J P 1981 *Phys. Rev. Lett.* **52** 287
Frenkel D and Smit B 2002 *Understanding Molecular Simulation, from Algorithms to Applications* 2nd edn (New York: Academic)
Galindo A, Jackson G and Photinos D 2000 *Chem. Phys. Lett.* **66** 631
Gay J G and Berne B J 1981 *J. Chem. Phys.* **74** 3316
Gil-Villegas A, McGrother S C and Jackson G 1997a *Mol. Phys.* **92** 723
Gil-Villegas A, McGrother S C and Jackson G 1997b *Chem. Phys. Lett.* **269** 441
Glaser M A 2000 *Advances in the Computer Simulation of Liquid Crystals* ed C Pasini and C Zannoni (Dordrecht: Kluwer) chapter 11 p 263
Goldstein H, Poole C and Safco J 2002 *Classical Mechanics* (Reading, MA: Addison-Wesley)
Gonin D and Windle A 1997 *Liq. Cryst.* **23** 489
Gonzalez-Segredo N and Coveney P V 2004 *Phys. Rev.* E **69** 061501
Gunstensen A K, Rothman D H, Zaleski S and Zanetti G 1991 *Phys. Rev.* A **43** 4320
Gwóźdź E, Bródka A and Pasterny K 1997 *Chem. Phys. Lett.* **267** 557
Halperin B I and Nelson D 1998 *Phys. Rev. Lett.* **41** 121
Hammond L A, Halliday I, Care C M and Stevens A 2002 *J. Phys. A: Math. Gen.* **35** 9945
Hashim R, Luckhurst G R, Prata F and Romano S 1993 *Liq. Cryst.* **15** 283
Hashim R, Luckhurst G R and Romano S 1986 *Liq. Cryst.* **1** 133
Hashim R, Luckhurst G R and Romano S 1990 *Proc. R. Soc. Lond. A: Math. Phys. Eng. Sci.* **429** 323
Hashim R and Romano S 1999 *Int. J. Mod. Phys.* B **13** 3879
He A, Zou Q, Luo L S and Dembo M 1997 *J. Stat. Phys.* **87** 115
He X and Luo L S 1997 *Phys. Rev.* E **56** 6811
Hess S 1975 *Z. Naturf.* a **30** 728
Hoogerbrugge P J and Koelman J M V A 1992 *Eur. Phys. Lett.* **19** 155
Hou S, Zou Q, Chen S, Doolen G D and Cogley A C 1995 *J. Comp. Phys.* **118** 329
Houssa M, McGrother S C and Rull L F 1999 *Comput. Phys. Commun.* **122** 259
Houssa M, Rull L F and McGrother S C 1998 *J. Chem. Phys.* **109** 9529
Huang S L and Bhethanabotla V R 1999 *Int. J. Mod. Phys.* C **10** 361
James R, Fernandez F A, Day S E, Komarcevic M and Crossland W A 2004 *Mol. Cryst. Liq. Cryst.* **422** 209
Johnston S J, Low R J and Neal M P 2002 *Phys. Rev.* E **65** 051706
Jung J, Denniston C, Orlandini E and Yeomans J M 2003 *Liq. Cryst.* **30** 1455
Koda T, Numajiri M and Ikeda S 1996 *J. Phys. Soc. Japan* **65** 3551
Koponen A, Kataja M and Timonen J 1998 *Int. J. Mod. Phys.* C **9** 1505
Krieger T J and James H M 1954 *J. Chem. Phys.* **22** 796
Kum O, Hoover W G and Posch H A 1995 *Phys. Rev.* E **52** 4899
Kumar S 2001 *Liquid Crystals* (Cambridge: Cambridge University Press)
Kushick J and Berne B J 1973 *J. Chem. Phys.* **59** 3732
Kuzuu N and Doi M 1983 *J. Phys. Soc. Japan* **52** 3486
Ladd A J C and Verberg R 2001 *J. Stat. Phys.* **104** 1191
Lansac Y, Glaser M A and Clark N A 2001 *Phys. Rev.* E **64** 051703
Lansac Y, Maiti P K, Clark N A and Glaser M A 2003 *Phys. Rev.* E **67** 011703
Lebwohl P A and Lasher G 1972 *Phys. Rev.* A **6** 426
Lebwohl P A and Lasher G 1973 *Phys. Rev.* A **7** 2222
Leslie F M 1979 *Adv. Liq. Cryst.* **4** 1
Levine Y K, Gomes A E, Martins A F and Polimeno A 2005 *J. Chem. Phys.* **122** 144902
Lishchuk S V and Care C M 2004 *Phys. Rev.* E **70** 011702

Lishchuk S V, Care C M and Halliday I 2004 *J. Phys.: Condens. Matter* **16** S1931
Luckhurst G R and Romano S 1980 *Mol. Phys.* **40** 129
Luckhurst G R and Romano S 1981 *Proc. R. Soc. Lond.* A **373** 111
Luckhurst G R and Romano S 1997 *J. Chem. Phys.* **107** 2557
Luckhurst G R and Simmonds P S J 1993 *Mol. Phys.* **80** 233
Luckhurst G R, Stephens R A and Phippen R W 1990 *Liq. Cryst.* **8** 451
Madsen L A, Dingemans T J, Nakata M and Samulski E T 2004 *Phys. Rev. Lett.* **92** 145505
Maier W and Saupe S 1958 *Z. Naturf.* a **13** 564
Maier W and Saupe S 1959 *Z. Naturf.* a **14** 882
Maier W and Saupe S 1960 *Z. Naturf.* a **15** 287
Maiti P K, Lansac Y, Glaser M A and Clark N A 2004 *Phys. Rev. Lett.* **92** 025501
Marenduzzo D, Orlandini E and Yeomans J M 2003 *Eur. Phys. Lett.* **64** 406
McBride C and Vega C 2002 *J. Chem. Phys.* **117** 10370
McDonald A J 2002 Computer simulation of liquid crystals *PhD Thesis* University of Bristol
McDonald A J and Hanna S 2004 *Mol. Cryst. Liq. Cryst.* **413** 135
McGrother S C, Gil-Villegas A and Jackson G 1996a *J. Phys. Condens. Matter* **8** 9649
McGrother S C, Gil-Villegas A and Jackson G 1998 *Mol. Phys.* **95** 657
McGrother S C, Sear R P and Jackson G 1997 *J. Chem. Phys.* **106** 7315
McGrother S C, Williamson D C and Jackson G 1996b *J. Chem. Phys.* **104** 6755
Memmer R 2000a *Liq. Cryst.* **27** 533
Memmer R 2000b *Mol. Phys.* **29** 483
Memmer R 2001 *J. Chem. Phys.* **114** 8210
Memmer R and Janssen F 1998a *J. Chem. Soc.: Faraday Trans.* **94** 267
Memmer R and Janssen F 1998b *Liq. Cryst.* **24** 805
Memmer R and Janssen F 1999 *Z. Naturf.* a **54** 747–54
Memmer R, Kuball H G and Schonhofer A 1993 *Liq. Cryst.* **15** 345
Mills S J and Cleaver D J 2000 *Mol. Phys.* **98** 1379
Monaghan J J 1992 *Ann. Rev. Astron. Astrophys.* **30** 543
Neal M P and Parker A J 1998 *Chem. Phys. Lett.* **294** 277
Neal M P and Parker A J 2000 *Phys. Rev.* E **63** 011706
Neal M P, Parker A J and Care C M 1997 *Mol. Phys.* **91** 603
Olmsted P D and Goldbart P M 1990 *Phys. Rev.* A **41** 4578
Onsager L 1949 *Ann. N.Y. Acad. Sci.* **51** 627
Osipov M A and Terentjev E M 1989 *Phys. Lett.* A **134** 301
Padilla P and Velasco E 1997 *J. Chem. Phys.* **106** 10299
Pagonabarraga I and Frenkel D 2001 *J. Chem. Phys.* **115** 5015
Paolini G V, Ciccotti G and Ferrario M 1993 *Mol. Phys.* **80** 297
Pasini P, Chiccoli C and Zannoni C 2000a *Advances in the Computer Simulation of Liquid Crystals* ed C Pasini and C Zannoni (Dordrecht: Kluwer) chapter 5 p 99
Pasini P, Chiccoli C and Zannoni C (ed) 2000b *Advances in the Computer Simulation of Liquid Crystals* (Dordrecht: Kluwer)
Perram J W and Wertheim M S 1985 *J. Comput. Phys.* **58** 409
Perram J W, Wertheim M S, Lebowitz J L and Williams G O 1984 *Chem. Phys. Lett.* **105** 277
Picken S J, Van Gunsteren W F, Van Duijnen P T and De Jeu W H 1989 *Liq. Cryst.* **6** 357
Polson J M and Burnell E E 1997 *Chem. Phys. Lett.* **281** 207
Qian T and Sheng P 1998 *Phys. Rev.* E **58** 7475
Qian Y H, d'Humieres D and Lallemand P 1992 *Europhys. Lett.* **17** 479
Rapaport D C 1995 *The Art of Molecular Dynamics Simulation* (Cambridge: Cambridge University Press)
Rey A D 2001 *Liq. Cryst.* **28** 549
Rigby M 1989 *Mol. Phys.* **68** 687
Romano S 1994 *Liq. Cryst.* **16** 1015
Romano S 2004a *Physica A* **337** 505
Romano S 2004b *Phys. Lett.* A **333** 110
Rull L F 1995 *Physica* A **220** 113
Sarman S 1996 *J. Chem. Phys.* **104** 342
Satoh K, Mita S and Kondo S 1996a *Liq. Cryst.* **20** 757
Satoh K, Mita S and Kondo S 1996b *Chem. Phys. Lett.* **255** 99
Shan X W and Chen H D 1993 *Phys. Rev.* E **47** 1815

Sluckin T J, Dunmur D A and Stegemeyer H 2004 *Crystals that Flow: Classic Papers from the History of Liquid Crystals* (London: Taylor and Francis)
Sollich H, Baalss D and Hess S 1989 *Mol. Cryst. Liq. Cryst.* **168** 189
Sonnet A M, Maffettone P L and Virga E G 2004 *J. Non-Newt. Fluid Mech.* **119** 51
Spencer T J and Care C M 2005 in preparation
Stelzer J, Berardi R and Zannoni C 1999 *Chem. Rev. Lett.* **299** 9
Stewart I 2003 *The Static and Dynamic Continuum Theory of Liquid Crystals: A Mathematical Introduction* (London: Taylor and Francis)
Stone A J 1978 *Mol. Phys.* **36** 241
Stroobants A 1992 *Phys. Rev. Lett.* **69** 2388
Stroobants A, Lekkerkerker H N W and Frenkel D 1986 *Phys. Rev. Lett.* **57** 1452
Succi S 2001 *The Lattice Boltzmann Equation for Fluid Mechanics and Beyond* (Oxford: Clarendon)
Svensek D and Zumer S 2002 *Phys. Rev.* E **66** 021712
Swift M R, Orlandini E, Osborn W R and Yeomans J M 1996 *Phys. Rev.* E **54** 5041
Toth G, Denniston C and Yeomans J M 2002a *Phys. Rev. Lett.* **88** 105504
Toth G, Denniston C and Yeomans J M 2002b *Comput. Phys. Comm.* **147** 7
Toth G, Denniston C and Yeomans J M 2003 *Phys. Rev.* E **67** 051705
Tschierske C 2001 *J. Mater. Chem.* **11** 2647
van Duijneveldt J S and Allen M P 1997 *Mol. Phys.* **92** 855
Varga S and Jackson G 2003 *Chem. Phys. Lett.* **377** 6
Veerman J A C and Frenkel D 1990 *Phys. Rev.* A **41** 3237
Veerman J A C and Frenkel D 1992 *Phys. Rev.* A **45** 5632
Velasco E and Mederos L 1998 *J. Chem. Phys.* **109** 2361
Vertogen G and de Jeu W H 1988 Thermotropic liquid crystals fundamentals *Chemical Physics* vol 45 (Berlin: Springer) chapter 8
Vieillard-Baron J 1972 *J. Chem. Phys.* **56** 4729
Vieillard-Baron J 1974 *Mol. Phys.* **28** 809
Wall G D and Cleaver D J 1997 *Phys. Rev.* E **56** 4306
Weeks J D, Chandler D and Anderson H C 1971 *J. Chem. Phys.* **54** 5237
Wei D Q and Patey G N 1992a *Phys. Rev.* A **46** 7783
Wei D Q and Patey G N 1992b *Phys. Rev. Lett.* **68** 2043
Weis J J, Levesque D and Zarragoicoechea G J 1992 *Phys. Rev. Lett.* **69** 913
Whittle M and Masters A J 1991 *Mol. Phys.* **72** 247
Williamson D C and Jackson G 1998 *J. Chem. Phys.* **108** 10294
Wilson M R 1999 *Struct. Bond.* **94** 42
Wilson M R and Allen M P 1991 *Liq. Cryst.* **12** 157
Wilson M R and Allen M P 1993 *Mol. Phys.* **80** 277
Withers I M 2003 *J. Chem. Phys.* **119** 10209
Withers I M, Care C M and Cleaver D J 2000 *J. Chem. Phys.* **113** 5078
Withers I M, Care C M, Neal M P and Cleaver D J 2002 *Mol. Phys.* **100** 1911
Wood E L, Bryan-Brown G P, Brett P, Graham A, Jones J C and Hughes J R 2000 *Proc. SID* **31** 124
Xu J, Selinger R L B, Selinger J V, Ratna B R and Sashidhar R 1999 *Phys. Rev.* E **60** 5584
Yarmolenko V 2003 Lattice modelling of liquid crystal mixtures *PhD Thesis* Sheffield Hallam University
Yoneya M and Iwakabe Y 1995 *Liq. Cryst.* **18** 45
Yoon S H, Lee C S, Yoon S I, Lee J H, Yoon H J, Choi M W, Kim J W and Won T 2004 *Mol. Cryst. Liq. Cryst.* **413** 2469
Zannoni C 1979 *Molecular Physics of Liquid Crystals* (New York: Academic) chapter 9 p 19
Zannoni C 2000 *Advances in the Computer Simulation of Liquid Crystals* ed C Pasini and C Zannoni (Dordrecht: Kluwer) chapter 2 p 17
Zannoni C 2001 *J. Mater. Chem.* **11** 2646
Zasadzinski J A N and Meyer R B 1986 *Phys. Rev. Lett.* **56** 636
Zewdie H 1998a *Phys. Rev.* E **57** 1793
Zewdie H 1998b *J. Chem. Phys.* **108** 2117
Zhang Z, Mouritsen O G and Zuckermann M J 1992 *Phys. Rev. Lett.* **69** 2803